

UC Davis

UC Davis Previously Published Works

Title

Automated analysis of lateral river connectivity and fish stranding risks. Part 2: Juvenile Chinook salmon stranding at a river rehabilitation site

Permalink

<https://escholarship.org/uc/item/91q918f6>

Journal

Ecohydrology, 14(6)

ISSN

1936-0584 1936-0592

Authors

Larrieu, Kenneth G
Pasternack, Gregory B

Publication Date

2021-05-14

DOI

10.1002/eco.2303

Data Availability

The data associated with this publication are available upon request.

Peer reviewed

1 **Automated analysis of lateral river connectivity and fish stranding risks. Part 2:**
2 **Juvenile Chinook salmon stranding at a river rehabilitation site**

3

4 Running head: Salmon stranding at rehabilitation site

5

6 **Kenneth G. Larrieu^a and Gregory B. Pasternack^{b*}**

7

8 *^aDepartment of Land, Air, and Water Resources, University of California at Davis, One*

9 *Shields Avenue, Davis, CA 95616-8626, USA; voice: (530) 302-5658; email:*

10 *kglarrieu@ucdavis.edu; ORCID 0000-0003-1706-3879*

11 *^bDepartment of Land, Air, and Water Resources, University of California at Davis, One*

12 *Shields Avenue, Davis, CA 95616-8626, USA; voice: (530) 302-5658; email:*

13 *gpast@ucdavis.edu; ORCID 0000-0002-1977-4175*

14

15 **Corresponding Author*

16

17 Cite as: Larrieu, K. G., Pasternack, G. B. 2021. Automated analysis of river habitat
18 connectivity and fish stranding risks. Part 2: Juvenile Chinook salmon stranding at a
19 river rehabilitation site. *Ecohydrology*. e2303. doi: 10.1002/eco.2303.

20

21 Abstract

22 The dynamics of fish stranding have not been academically investigated within the
23 context of physical adjustments to rivers for habitat enhancement purposes. River
24 projects may aim to help fish populations but instead may function as attractive
25 nuisances reducing populations because of unaccounted-for stranding risk. This
26 study applies a novel algorithm to predict spatially explicit, meter-resolution fish
27 stranding risk at a river rehabilitation site in California to address three scientific
28 questions. Post-project disconnected wetted area predictions were validated
29 against water surface elevation measurements and time lapse photography of flow
30 reductions and stranding events. Comparison of pre-project, final design, and post-
31 project topographies revealed that occurrence and severity of stranding events is
32 highly sensitive to side-channel topographic structure and post-project
33 morphodynamic change. Even with moderate flows, side channel exits tend to
34 close off by bars built across them via bedload transport. Implications for river
35 management practices and river rehabilitation project design are discussed.

36 Keywords: fish stranding, river restoration, hydraulic connectivity, ecohydraulics,
37 rearing habitat, regulated rivers

38

39 1. Introduction

40 At the global scale, rivers and the ecosystems they support are adversely impacted
41 by anthropogenic disturbances that include flow diversions and alterations, blockage of
42 streams to fish passage, channel geometry simplification, sediment supply modification,
43 and water quality degradation (Meybeck, 2003). In California, as elsewhere in the world,
44 such impacts have caused widespread collapse of freshwater and anadromous fish
45 populations (Moyle et al., 2011). Problem acknowledgement has motivated mitigation,
46 including by restoring, rehabilitating, or enhancing degraded riverine habitats. Such
47 projects have yielded mixed results (Kauffman et al., 1997; Palmer et al., 2010; Morandi
48 et al., 2014), necessitating significant improvements to river restoration project design
49 (Brown et al., 2015; Brown and Pasternack, 2019) and pre- and post-construction
50 design evaluation (Brown and Pasternack, 2009; Schwindt et al., 2020).

51 1.1. Fish stranding at restoration sites?

52 In the companion article (Larrieu et al., 2020), a thorough literature review was
53 presented about the scope of fish stranding as an ecological process and river
54 management problem. The topic of fish stranding has not been academically
55 investigated within the context of the burgeoning literature about active and passive
56 physical and vegetative adjustments to rivers for environmental stewardship, whether
57 termed restoration, rewilding, rehabilitation, mitigation, or enhancement. Documented
58 consequences of stranding for individual fish are numerous and wide-ranging, from
59 temporary stress response to mortality (Bauersfeld, 1978; Cushman, 1985; Sabo et al.,
60 1999; Quinn and Buck, 2001; Flodmark et al., 2002; Evans, 2007).

61 Conceptually, the very areas that are most prone to stranding are often of greatest
62 interest in re-engineering (Rosenfeld et al., 2008; Paillex et al., 2009; Person, 2013;
63 Erwin et al., 2017). Stranding may be interstitial (also called bar stranding or beaching)
64 or pool (also called off-channel stranding, isolation, or trapping) (Hunter, 1992). Large
65 side channels and floodplain habitat features are notorious for increased interstitial and
66 pool stranding risks, yet such areas can also function as ideal habitat with abundant
67 food and cover for rearing juvenile salmonids, resulting in higher growth rates compared
68 to rearing juveniles that do not utilize floodplain habitat (Sommer et al., 2005). It is
69 unknown whether these benefits outweigh detrimental fish stranding.

70 The relative degree of these effects is expected to be highly dependent on specific
71 physical site characteristics. Factors relevant to fish stranding include topography,
72 ramping rate (rate of water surface elevation change), water temperature, time of day,
73 and wetted history (length of time at sustained discharge before flow reduction occurs)
74 (Bradford, 1997; Halleraker et al., 2003; Irvine et al., 2014; Auer et al., 2017).
75 Historically, fish population resilience hinged on a fecundity-based life strategy, yielding
76 resilience against these physical factors. Today, many fish populations are so small and
77 large fractions of these remaining populations can be so highly attracted to restored
78 sites (e.g., Elkins et al., 2007; Harrison et al., 2019) that such populations may be
79 extremely sensitive to stranding risk. It should also be noted that the majority of
80 stranding studies are concerned with juvenile salmonids, and the influence of physical
81 factors on fish stranding may vary significantly for other species and lifestages.

82 1.2. Design-phase stranding prediction

83 Although many scientists report that project monitoring is neglected after river

84 projects are constructed, design (including quantitative design stress testing) is
85 arguably the most neglected project phase (Wheaton et al., 2004; Pasternack and
86 Brown, 2013). Traditionally, baseline characterization and post-project appraisal involve
87 empirical methods that cannot be applied to “virtual” (i.e., on computer only) designs.
88 However, modern mechanistic modeling works equally well on real and virtual cases.
89 The grand challenge of river restoration in the 21st century is to develop and apply
90 comprehensive eco-geomorphic mechanistic models that enable pre-construction
91 design testing, including automated design optimization for different eco-geomorphic
92 objectives (Pasternack, 2020).

93 A variety of methodologies have been presented in the literature for quantifying
94 stranding risks with hydrodynamic models that could be used in all river project phases
95 (Noack and Schneider, 2009; Richmond and Perkins, 2009; Tuhtan et al., 2012; Noack
96 et al., 2013; Hauer et al., 2014; Vanzo et al., 2016; Juárez et al., 2019). These stranding
97 assessment methodologies have not yet been adopted by the larger scientific and
98 management communities to aid design of environmental flow regimes and river
99 restoration projects. Demonstration of predictive success will be needed to stimulate
100 wider use, as none of the current stranding risk assessment methodologies validate
101 predicted locations and severity of stranding risk using field observations, limiting
102 confidence in their usefulness and interpretability. Such validation can prove quite
103 difficult in practice. While this study achieved good qualitative agreement with predicted
104 and observed stranding events, insufficient data were collected to enable a thorough
105 quantitative validation (e.g. exact numbers of stranded fish and stranding absence were
106 not documented).

107 1.3. Study purpose

108 The companion article (Larrieu et al., 2020) presented a novel fish stranding
109 algorithm that could be suitable for use in real river assessment and virtual design
110 testing. In contrast to existing methods, this algorithm employs a graph-theoretic
111 approach to 2D hydrodynamic model outputs to quantify lateral habitat connectivity for
112 any fish species/life stage of interest. The algorithm further produces several metrics
113 relevant to pool stranding for a given downramping scenario, including explicit spatial
114 mapping of disconnection events, discharges at which disconnections occur,
115 disconnection frequency, and more.

116 This study evaluated the accuracy of that algorithm for a test case and then used
117 findings to answer three fundamental scientific questions about the roles of topography
118 and ramping rate on fish stranding (Table 1). A river rehabilitation project in a regulated
119 river canyon in north central California (Yuba Canyon Project, described later) was
120 selected as the test site. Site features included constructed side channels, riffles, and
121 bars. The site also underwent modest subsequent morphodynamic processes that
122 quickly enhanced stranding risk. Juvenile Chinook salmon was the species and
123 lifestage of interest. This study investigated pool stranding risks for isolating topographic
124 saddles at 0.91 m (3 ft) resolution. Results of stranding risk analyses were compared
125 with field observations to the extent possible to evaluate its efficacy as well as its
126 limitations.

127

128 Table 1. Experimental design for answering scientific questions in the case study.

Question	Test methods	Test metrics
Can steady-state 2D hydrodynamic models accurately predict the occurrence of disconnected riverine habitat during flow reductions?	Apply interpolation and path-finding algorithm to incremental steady-state discharge models.	Comparison of predicted disconnecting areas and corresponding discharges with those indicated by gage data and time-lapse video.
How do constructed and natural topographic changes at the test site affect fish stranding risks?	Apply habitat suitability functions to model-derived disconnected areas, link disconnecting discharges to frequency with gage data.	Changes in disconnected habitat area for characteristic flow reduction, disconnection frequency.
How much does ramping rate influence juvenile Chinook stranding risks at the test site?	Quasi-unsteady ramping rate estimation.	Comparison of ramping rate estimates with target values identified in literature.

129

130 2. Fish stranding risk algorithm

131 The companion article (Larrieu et al., 2020) presented a new methodology that
 132 characterizes fish stranding risks for a given topography, target species/lifestage, and
 133 flow ramping scenario. The concepts detailed in the companion article are briefly
 134 summarized here and illustrated with a flowchart (Figure 1). The free, open-source
 135 algorithm is implemented as part of River Architect (Schwindt et al., 2020;
 136 <https://riverarchitect.github.io/>).

137 The methodology requires modern 2D ecohydraulic data inputs and then produces
 138 2D hydraulic disconnection and fish stranding risk maps and associated aggregate
 139 metrics. It does not matter what 2D model is used, as long as the digital elevation model

140 (DEM), water surface elevation (WSE), depth, velocity magnitude, and velocity angle
141 results for each discharge are available as raster data. Users also optionally supply
142 habitat suitability curves, and associated non-hydraulic habitat rasters that present the
143 spatial distributions of conditions such as substrate, cover, and water temperature.
144 There are six user-specified parameters and the user selects the water surface
145 elevation interpolation/extrapolation method.

146 A wetted area is considered disconnected from the mainstem of the river channel
147 during a flow reduction from Q_{high} to Q_{low} if it is not possible for fish of the
148 species/lifestage of interest to reach the main channel from that area at one or more
149 discharge Q_i . In this study, this definition is applied at the resolution of the
150 hydrodynamic model and underlying DEM. The terms pool stranding and isolation
151 apply, not at the classic morphological unit scale, but at the raster resolution scale. An

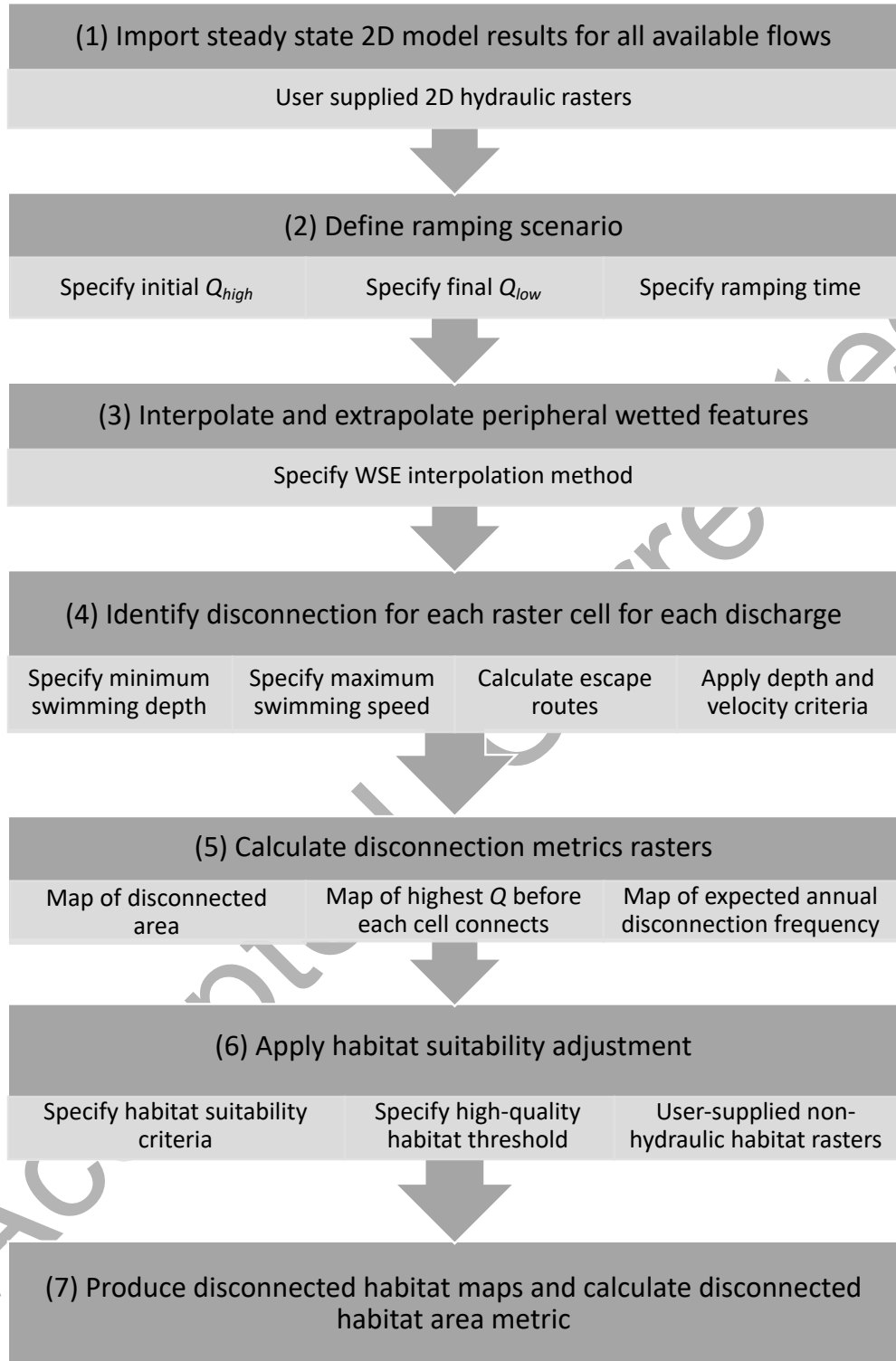


Figure 1. Fish stranding algorithm workflow phases, including required user inputs, key steps, and outputs.

152 area may be considered disconnected not only in the case of physically separate wetted
153 areas, but also if low depth or high velocity barriers are present preventing individuals
154 from moving into the main channel.

155 For the purpose of identifying disconnected areas, the main channel is defined as
156 the largest continuous wetted area deeper than the minimum swimming depth threshold
157 at the final, low discharge. This definition implies that if a fish reaches the main channel,
158 it will not become stranded within that area (for the applied downramping scenario).

159 Graph representation of river navigability from any initial wetted cell to the main channel
160 was achieved using Dijkstra's path-finding algorithm, which enables characterization of
161 fish movement options (Dijkstra, 1959; McElroy et al., 2012; Etherington, 2016). Nodes
162 for which no path exists back into the main channel at a given discharge are considered
163 disconnected. Outputs include a disconnected area map for each discharge, a map of
164 the highest discharge at which each cell disconnects, and a map of the average number
165 of times per year that flows drop below the disconnection discharge in each cell.
166 Results may be subset to a seasonal window to align with ecological timing.

167 Disconnection discharge and frequency rasters are helpful in identifying areas with
168 potential stranding risks, but actual stranding also necessitates fish presence. Habitat
169 suitability modeling (Pasternack, 2019) serves as a proxy for fish presence likelihood
170 and abundance in an area preceding a disconnection event. Computed combined
171 habitat suitability index rasters are used to weight disconnected area to produce a
172 "disconnected habitat" raster. In addition to a spatially explicit map of disconnected
173 habitat for the applied downramping scenario, a summary metric herein referred to as
174 disconnected habitat area (DHA) is computed to indicate the total amount of high-

175 quality fish habitat disconnected by flow reduction (see Larrieu et al., 2020).

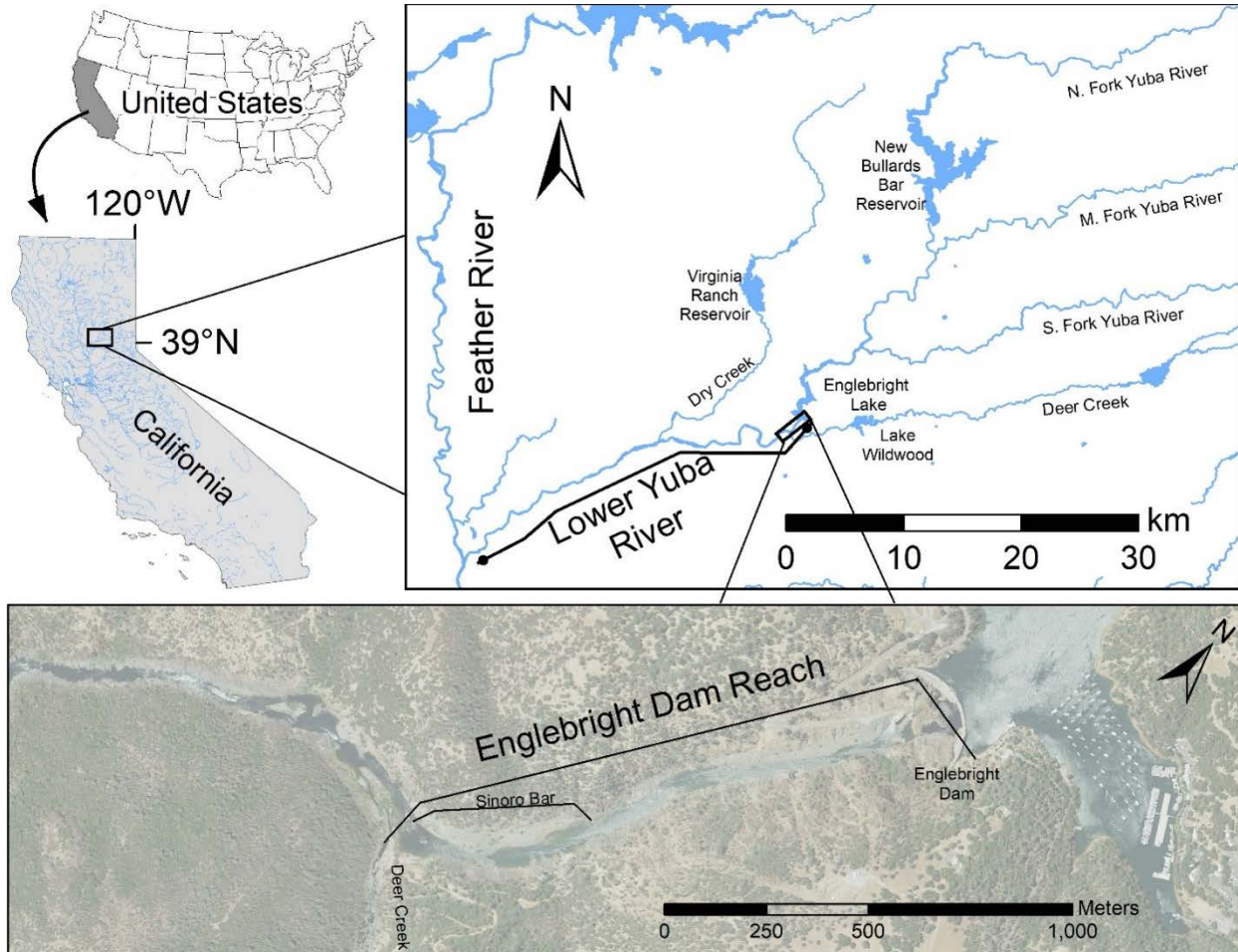
176 3. Study setting

177 3.1. Yuba River

178 The Yuba River catchment drains 3,490 km² of the western Sierra Nevada
179 mountains (Figure 2). Salmon were once so abundant that Native Americans would
180 spear them "by the hundred" (Chamberlain and Wells, 1879). During California's gold
181 rush miners diverted the river to blast gold-laden hillsides. Released mercury-
182 contaminated sediments filled the valley 6-24 m high (Yoshiyama et al., 1998). This
183 prompted dam construction, including 79-m high Englebright Dam that marks the
184 upstream limit of anadromous salmonid migration. Though salmon have lost access to
185 73% of their historical Yuba habitat area, Englebright Dam holds back ~ 22 million m³ of
186 sediment, preventing further harmful sediment fluxes and enabling ecogeomorphic
187 recovery downstream (Snyder et al., 2004; Pasternack et al., 2010).

188 The ~ 37.5-km long gravel-cobble lower Yuba River (LYR) spans from Englebright
189 Dam to the confluence with the Feather River. It constitutes the remaining area of
190 accessible Chinook salmon and steelhead habitat. It is inhabited by federally threatened
191 spring-run Chinook salmon (*Oncorhynchus tshawytscha*) and Central Valley steelhead
192 (*Oncorhynchus mykiss*). It is designated as critical habitat for both species. Current
193 management includes systemic, repeated mapping, monitoring, and mechanistic
194 modeling that supports habitat enhancement projects throughout the LYR.

195



196

197 Figure 2. Englebright Dam Reach of the lower Yuba River. The Yuba Canyon Project is
 198 located at Sinoro Bar.

199 3.2. Flow operations

200 Flow regulations include monthly minimum flow requirements by water year type and
 201 specified rate of flow changes when flows are within the controllable range of $\leq 116 \text{ m}^3/\text{s}$
 202 (4,100 cfs). In addition to constraints on daily flow changes, proposed regulatory
 203 conditions require that the rate of flow increase not exceed $14.2 \text{ m}^3/\text{s}$ per hour (500
 204 cfs/hr), whereas the rate of flow decrease must not exceed $5.66 \text{ m}^3/\text{s}$ per hour (200
 205 cfs/hr) during the fry and juvenile rearing season (FERC, 2019).

206 To further address the concern of juvenile fish stranding, operators maintain an
207 objective of 2.83 m³/s per hour (100 cfs/hr) reductions under normal conditions, and
208 5.66 m³/s per hour (200 cfs/hr) when passing storm flows. The target rate of 2.83 m³/s
209 per hour is technically maintained when observed at an hourly timescale. However, 15-
210 minute resolution gage data in addition to 1-minute resolution time-lapse camera
211 observations made as part of this study indicate that the implementation of 2.83 m³/s
212 flow reductions typically occur during intervals of 20-30 minutes followed by constant
213 flows for the remainder of the hour, corresponding to a maximum instantaneous rate of
214 change in the range of 5.66-8.50 m³/s per hour (200-300 cfs/hr) (see supplementary
215 materials for examples). Thus, a downramping rate of 7.08 m³/s per hour (250 cfs/hr)
216 was determined to be representative of the greatest ramping experienced under current
217 operating procedures in regards to stranding risks, at least in the uppermost reaches
218 where hydraulic controls have not significantly attenuated the hydrograph wave.

219 3.3. Test site

220 The test site (Figure 2, Sinoro Bar) began 200 m downstream of the Narrows 1
221 powerhouse in the geomorphically delineated Englebright Dam Reach (EDR) and
222 ended 400 m downstream of the onset of the Deer Creek confluence. The confined
223 bedrock canyon has low sinuosity, an average bankfull width of 59 m, and a mean slope
224 of 0.31%. Beginning in 2007, gravel/cobble augmentation has been regularly
225 implemented by the U.S. Army Corps of Engineers below Englebright Dam to ensure
226 availability of gravel substrate suitable for salmonid spawning (Pasternack et al., 2010).
227 As a result, substrate includes pre-existing bedrock, boulders, and angular shot rock
228 plus injected gravel and cobble.

229 To increase spring-run Chinook salmon habitat, the U.S. Fish and Wildlife Service's
230 Anadromous Fish Restoration Program and its contractors designed and built a habitat
231 enhancement project called the "Yuba River Canyon Salmon Habitat Restoration
232 Project" (Yuba Canyon Project hereafter), completed summer 2018. An oversized
233 cobble point bar ("Sinoro Bar", a remnant from hydraulic mining sediment) was
234 terraformed to create two new large side channel features to serve as habitat for rearing
235 juvenile Chinook salmon. Excess bar sediment was pushed into the baseflow channel
236 to create spawning riffle habitat. Shortly thereafter in December 2018 side channels
237 were disconnecting from the mainstem. Fish biology experts reported the stranding of
238 an estimated 1,000 Chinook salmon juveniles on one occasion alone (PSMFC, 2019).
239 Stranding has been observed during subsequent disconnections.

240 **4. Methods**

241 4.1. Experimental design

242 This study was initiated after the site was built in response to disconnections and
243 fish stranding. Therefore, while monitoring of disconnection events and stranding was
244 conducted for the post-project condition, this was not possible for the pre-project
245 condition, and the virtual design was not observable. Further, the timing of real flow
246 ramping could not be controlled, as it hinged on rapidly-changing weather and reservoir
247 inflow. The Yuba Canyon site is remote and only accessible by hiking downcanyon. It is
248 ~ 2.5 hours from campus to field site, not counting prep time. This meant rapid
249 response to sudden downramping was impossible, except by fortuitous occurrence
250 during a site visit. Given this situation, the primary approach to address question 1
251 (Table 1) involved matching time lapse photography showing disconnections with 2D

252 hydrodynamic model visualizations of the same discharges.

253 The experimental design consisted of implementing the River Architect stranding
254 risk module for a constant setup in all aspects, except having three topographic
255 scenarios to address question 2 (Table 1). The assessment aimed to determine how
256 topographic modifications made as part of river rehabilitation measures (e.g., the
257 introduction of side channels) affect stranding risks for juvenile Chinook salmon. Key
258 metrics for evaluating changes in stranding risk between topographic conditions
259 included (i) the total amount of area disconnected under a characteristic ramping
260 scenario, (ii) the amount of disconnected habitat area for juvenile Chinook salmon, (iii)
261 the discharge at which potential stranding events occur, and (iv) the expected frequency
262 of such events during vulnerable lifestage periods.

263 4.2. Digital elevation models

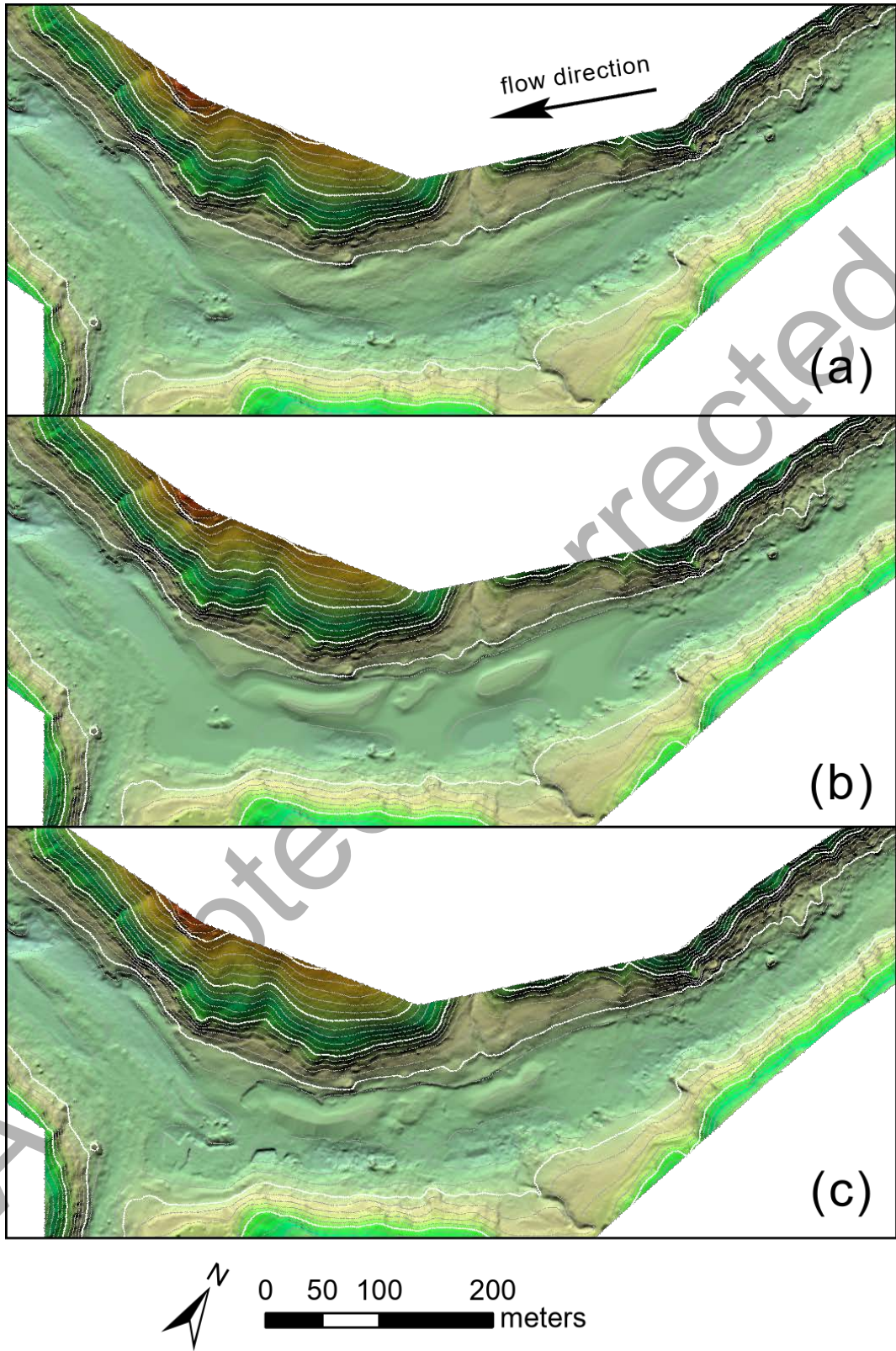
264 Meter-resolution DEMs were made for 2017 pre-project, final virtual design, and
265 2019 post-project conditions (Figure 3). The pre-project DEM was made from a
266 combination of near-infrared lidar, green lidar, and sonar data collected in late summer
267 2017 (Silva and Pasternack, 2018). The final virtual design DEM used for the Yuba
268 Canyon Project had been created by modifying the 2017 DEM to grade the main
269 channel and create two side channel features running through the point bar. The post-
270 project DEM was created by combining new sonar and RTK GPS data collected during
271 late summer 2019, a year after construction. The data from these 2019 surveys cover
272 most of the main channel, as well as the entire Yuba Canyon Project site domain.

273 4.3. Discharge data and ramping scenario

274 Discharge time series data were acquired to identify relevant ramping scenarios, set

275 model boundary conditions, and calculate rasters of the expected annual frequency of

Accepted, Corrected



276

277 Figure 3: Digital elevation models of (a) pre-project, (b) final design, and (c) post-project
 278 topography. Contour lines shown for 3.05-m (10-ft) elevation differences.

279 disconnection. Discharge data for the LYR near Smartsville was obtained from
280 Department of Water Resources' California Data Exchange Center (YRS gage). Deer
281 Creek inflow data was obtained from USGS gage #11418500.

282 This study's ramping scenario assessed stranding risks for a flow reduction from
283 56.6 to 14.2 m³/s (2,000 to 500 cfs) over 6 hours. It was representative of the typical
284 downramp during juvenile spring-run Chinook salmon rearing. Site stranding events
285 exhibit this scenario. The duration was chosen such that the rate of flow decrease (7.08
286 m³/s per hour, or 250 cfs/hr) is characteristic of those typically observed during the most
287 rapid regulated flow reductions on the LYR, as discussed in section 3.2.

288 4.4. Yuba Canyon project 2D model

289 Steady-state SRH-2D v. 2.2 (Lai, 2008) 2D hydrodynamic models were applied for
290 each topography with the same computational mesh (0.91-m (3-ft) node spacing),
291 model parameters (eddy viscosity coefficient of 0.1; spatially constant Manning's n of
292 0.055), and downstream boundary conditions (see supplementary materials) used in the
293 Yuba Canyon Project. Models were run for 14 LYR discharges from 14.2 to 56.6 m³/s
294 (500 to 2,000 cfs). The supplementary materials provide further details regarding model
295 boundary conditions, hydrodynamic model validation, accuracy of River Architect's
296 water surface extrapolation methods, and example downramping hydrographs in the
297 study reach.

298 4.5. Biological data

299 Moniz et al. (2019) developed and bioverified observation-based LYR habitat
300 suitability criteria functions for two size classes of rearing Chinook salmon and

301 steelhead. This study used their juvenile Chinook salmon functions to calculate
302 combined (geometric mean) depth and velocity habitat suitability indices in River
303 Architect. Though it is important (Moniz et al., 2019), cover was not accounted for in this
304 analysis mindfully to isolate the influence of altered morphology on stranding risks. Little
305 vegetative or streamwood cover exists in the recontoured terrain to make cover a factor
306 differentiating project stages.

307 Applied thresholds for minimum swimming depth and maximum swimming speed
308 were 6.1 cm (0.2 ft) and 58 cm/s (1.9 ft/s), respectively. These were estimated from fish
309 passage references (Bell, 1991; Katopodis and Gervais, 2016; CDFW, 2017). The
310 season of interest applied to compute the expected annual frequency of disconnection
311 was February 1 to June 15 (typical LYR Chinook salmon juvenile rearing period).

312 4.6. Time lapse photography

313 To aid assessment of disconnected area prediction, Browning Dark Ops Pro XD
314 Dual Lens 24 megapixel trail cameras were set to record time-lapse photography and
315 deployed to view each side channel's outlet. Downramping events evident in real-time
316 flow gages indicated potential periods of disconnection. When a disconnection was
317 manually found in an event photoset, time stamps enabled linking with the flow record
318 to estimate disconnection discharges. Photo time series were produced into videos.

319 **5. Results**

320 Methodological performance of interpolated and extrapolated peripheral wetted
321 features is reported in the supplementary materials. Testing the relative sensitivity of
322 stranding predictions to the depth and velocity criteria found that the velocity criterion is

323 expected to have little effect on restriction of juvenile Chinook movement in the study
324 area. This result was not surprising considering the relative swimming strength of
325 juvenile salmonids and that flow velocities were typically low in the side channel
326 features and shallow, low-grade areas most prone to disconnection. Nonetheless,
327 sensitivity to the velocity criterion may be greater in other areas with steeper slopes and
328 higher velocities near disconnecting areas.

329 Video comparison of both side channels disconnecting with modeled disconnection
330 events can be viewed at <https://vimeo.com/user120675722>.

331 5.1. Disconnected areas

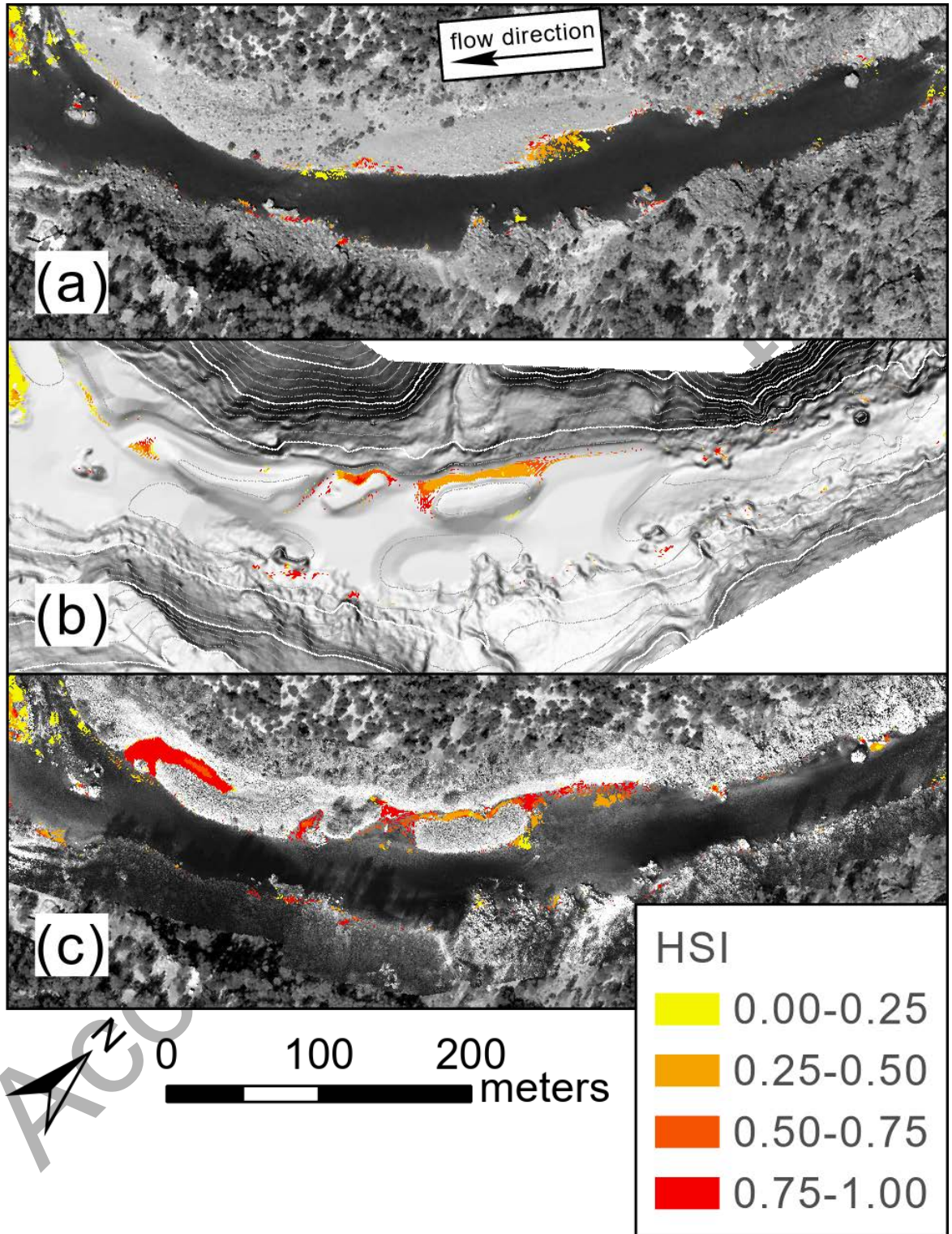
332 Disconnected habitat maps for the three topographic conditions illustrate a
333 significant difference between pre-project and post-project stranding risks (Figure 4).
334 While the constructed side channels in the post-project condition are of high habitat
335 quality, they are also the primary sources of disconnected habitat area within the model
336 domain for the applied downramping scenario.

337 Increases in disconnected area occur from the pre-project condition to project
338 design (7.7%) and from project design to post-project (26%) (Table 2, Figure 5).
339 Notably, the disconnected area is very fragmented with small patches in the pre-project
340 condition, but highly spatial coherent as large patches in the upper designed side
341 channel. They are even more abundant as large patches in the post-project condition.

342 Yet disconnected area does not tell the whole risk story, because DHA shows a
343 different result. For DHA, there is an 8.8% decrease from pre-project to design,
344 suggesting that the river might have had less stranding afterwards, even if it were more

345 concentrated in the side channel. However, construction resulted in a 207% increase in
346 DHA between design and post-project conditions. Put another way, doing the
347 restoration project tripled the amount of high-quality habitat area that becomes
348 disconnected during the applied flow reduction. This difference is primarily due to the

Accepted, Corrected



349

350 Figure 4. Disconnected area weighted by juvenile Chinook salmon combined habitat
 351 suitability indices for a flow reduction from 56.6 to 14.2 m³/s. Topographic conditions
 352 are (a) pre-project, (b) project design, and (c) post-project.

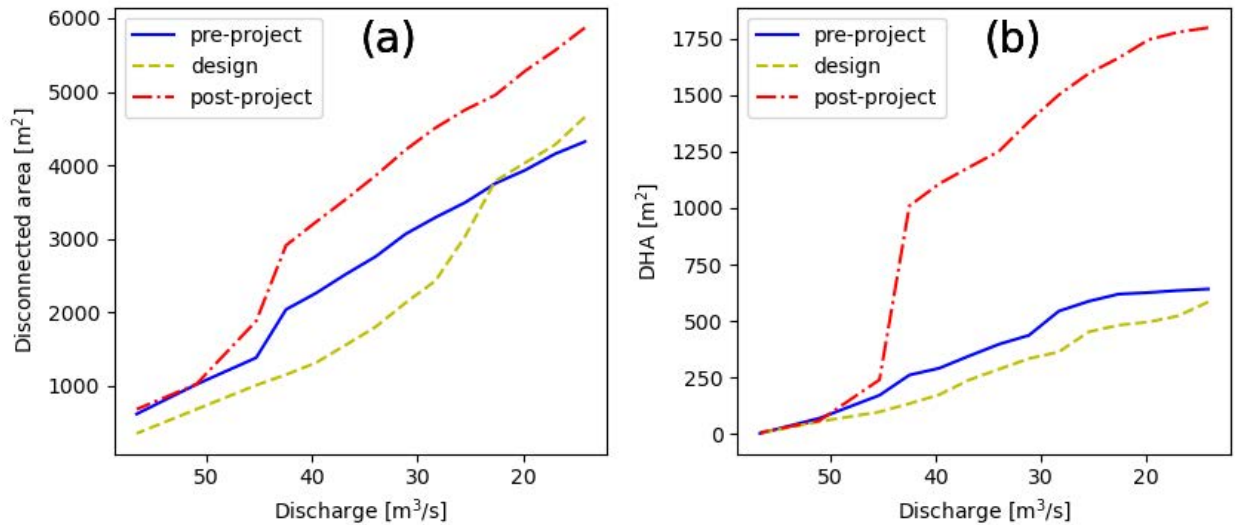
353

354 Table 2. Total disconnected area and disconnected habitat area for each of the
355 topographic conditions investigated.

Condition	Disconnected Area (m ²)	DHA (m ²)
Pre-project	4,321	642
Project design	4,656	585
Post-project	5,870	1,798

356

357 disconnection of the lower side channel (at the downstream end of Sinoro Bar) that
358 occurs for the post-project topography but was not predicted to occur for the project
359 design topography. In contrast, disconnection of the upper side channel was predicted
360 for the design topography. However, the upper side channel was not included in DHA
361 for the design topography as it was of moderate habitat suitability (0.25-0.75). In all
362 cases, DHA accounted for less than one third of the total disconnected area, indicating
363 that the majority of disconnected area does not fall within the highest habitat suitability
364 range of 0.75-1.



365

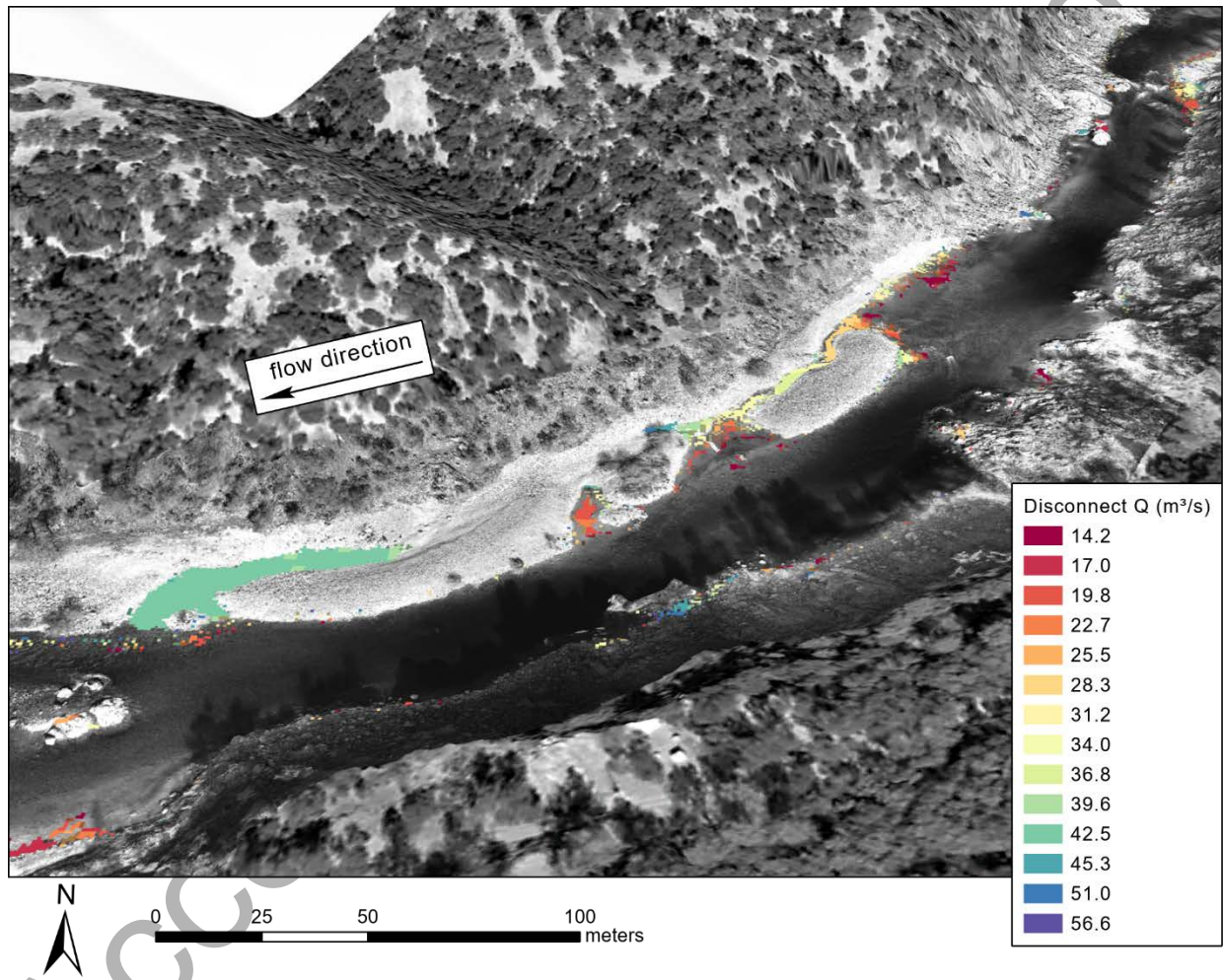
366 Figure 5. (a) Total disconnected area and (b) DHA for the applied flow reduction. Note
 367 discharge decreases along the horizontal axis.

368 A large portion of the baseline disconnected area for the pre-project condition is on a
 369 mid-channel bar downstream of the Deer Creek confluence. This disconnected area
 370 was persistent across all topographic scenarios. However, due to its location, it is more
 371 difficult to make definitive statements about its patterns of disconnections due to its
 372 location and resultant dependence on both Yuba River and Deer Creek flows. This
 373 landform has been subjected to many anthropogenic disturbances and modifications by
 374 instream gold miners and regulatory agencies. While the disconnecting area of this
 375 landform is included in Table 2, this area is not pictured in Figure 4 to focus
 376 visualization on the changes within the Yuba Canyon Project area.

377 5.2. Disconnecting discharges and disconnection frequency

378 Most disconnections were predicted to occur in the range of 42.45 m³/s (1,500 cfs)
 379 down to 28.31 m³/s (1,000 cfs), with relatively little area disconnecting over the rest of
 380 the modeled flow range (Figure 6). The lower side channel is estimated to become

381 disconnected for juvenile Chinook salmon at $\sim 42.45 \text{ m}^3/\text{s}$ causing a large increase in
382 DHA (Figure 5), while the upper side channel is expected to split into parts which
383 disconnect over a range of flows from $36.79 \text{ m}^3/\text{s}$ ($1,300 \text{ cfs}$) to $28.31 \text{ m}^3/\text{s}$. A few other
384 small pools and alcoves that become

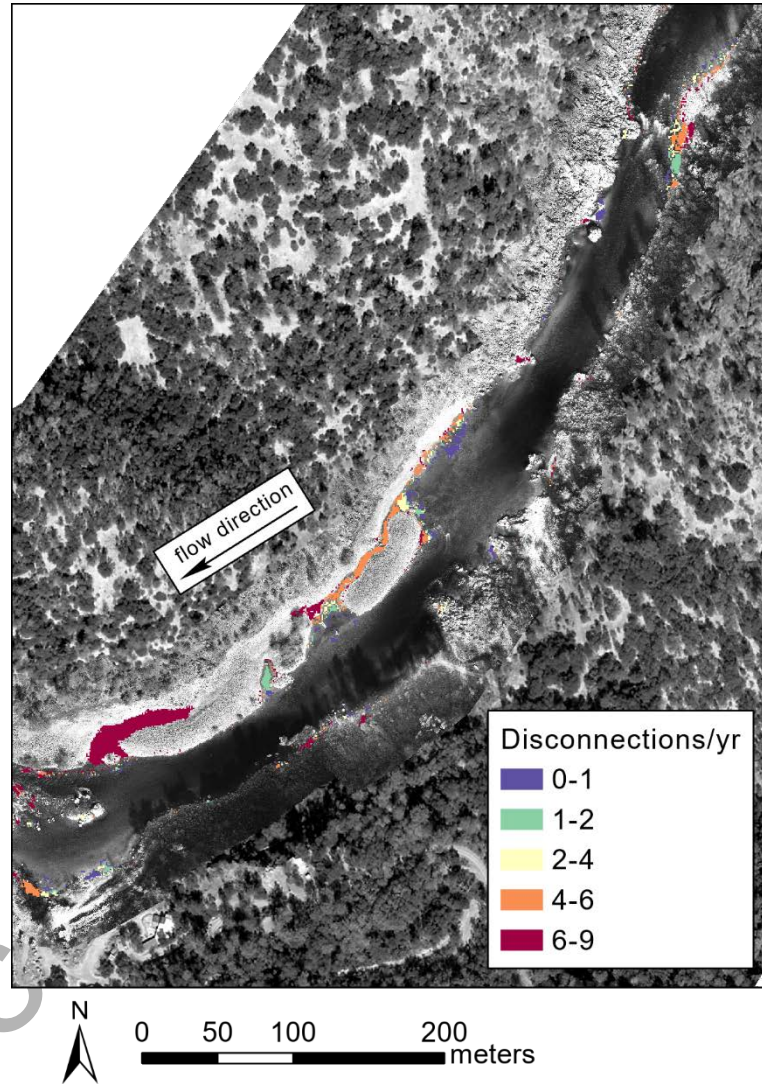


385
386 Figure 6. Disconnecting discharges for each area disconnected by a flow reduction from
387 56.6 to $14.2 \text{ m}^3/\text{s}$. Aerial imagery courtesy of Duane Massa.

388 disconnected are delineated between the two side channels as well as upstream of the
389 Yuba Canyon site.

390 Disconnection frequencies ranged from < 1 to ~ 9 disconnections per year during the

391 juvenile rearing season (Figure 7). Notably, the lower side channel is both the largest
392 source of DHA and predicted to have one of the highest disconnection frequencies. A
393 general trend exists between disconnecting discharge and disconnection



394
395 Figure 7. Disconnection frequency for the areas disconnected by a flow reduction from
396 56.6 to 14.2 m³/s. This calculation only considers disconnections occurring during the
397 applied season for juvenile Chinook rearing of Feb 1 - June 15.
398 frequency, with features disconnecting at lower discharges (Figure 6) also having lower
399 disconnection frequencies (Figure 7).

400 5.3. Ramping rate estimates

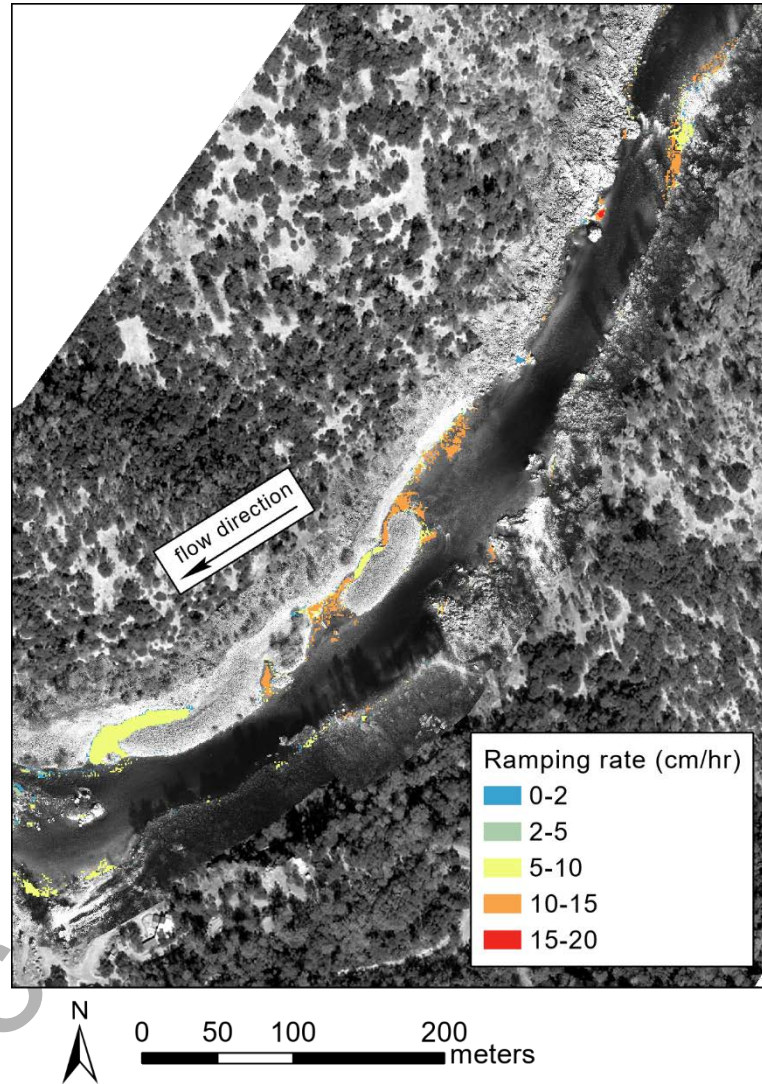
401 Ramping rate estimates range from 0-20 cm/hr, with the majority of disconnected
402 area at the Yuba Canyon site falling within the range of 5-15 cm/hr (2-5.9 in/hr) (Figure
403 8). For reference, using the stage-discharge relation for the applied downramping
404 scenario yields an average ramping rate of 11.26 cm/hr (4.43 in/hr), roughly
405 corresponding to the mid-range of the ramping rate estimates within disconnected
406 areas.

407 5.4. Disconnecting discharge prediction accuracy

408 The lower side channel was observed to disconnect at a flow of $\sim 42.45 \text{ m}^3/\text{s}$ (1,500
409 cfs) (Figure 9), the corresponding flow for which the side channel was predicted to
410 become effectively disconnected (Figure 6). While some hydraulically connected
411 interstitial areas were observed at $42.45 \text{ m}^3/\text{s}$, the water depth was below the minimum
412 swimming depth for juvenile Chinook salmon. Four subsequent visits were made to
413 monitor the site from late fall to spring 2019 when flows were below $42.45 \text{ m}^3/\text{s}$. On
414 every such occasion, the lower side channel was observed to be disconnected, while
415 dozens of juvenile salmon were observed to be trapped in the side channel.

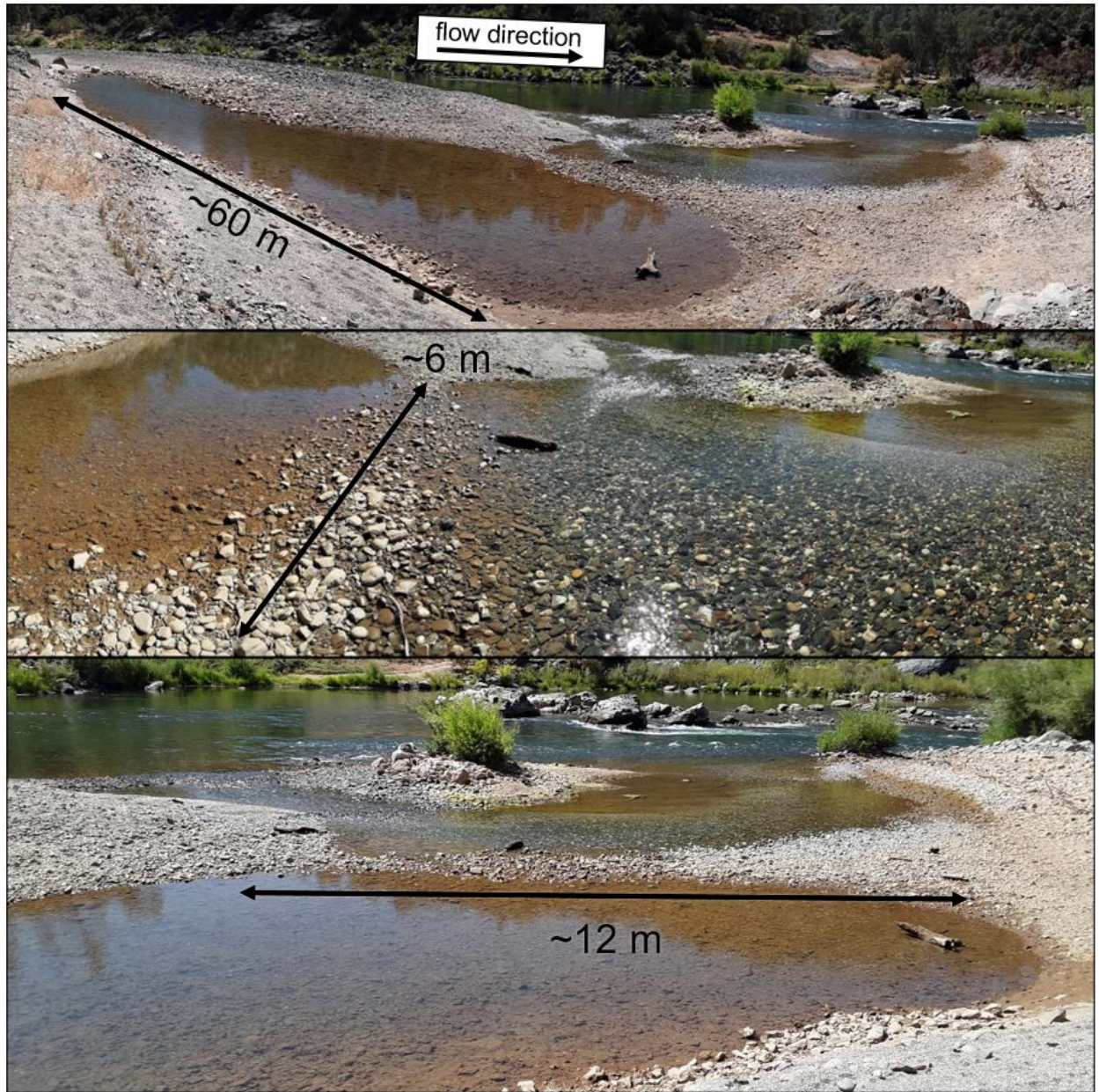
416 The upper side channel was predicted to disconnect in stages (Figure 6). At 56.6
417 m^3/s (2,000 cfs), it maintained connectivity at the inlet and outlet. Then, it was predicted
418 to separate at the midpoint into one section with a downstream connection and another
419 section with an upstream connection. Upon further flow recession, the lower half was
420 predicted to disconnect at $\sim 36.79 \text{ m}^3/\text{s}$ (1,300 cfs) followed by the upper half
421 disconnecting at $\sim 28.32 \text{ m}^3/\text{s}$. Field observations at a flow of $\sim 38.20 \text{ m}^3/\text{s}$ (1,350 cfs)
422 illustrated conditions in agreement with this predicted sequence of events (Figure 10).

423 Dozens of juvenile salmon were also observed in this side channel during visits made
424 as part of this study, in addition to the stranded juveniles observed in both side
425 channels in December 2018 (PSMFC, 2019).



426

427 Figure 8. Ramping rate estimates for the areas disconnected by a flow reduction from
428 56.6 to 14.2 m³/s over 6 hours.



429

430 Figure 9. Three perspectives of the lower side channel becoming disconnected from the
431 mainstem at $\sim 42.45 \text{ m}^3/\text{s}$.



432

433 Figure 10. The upper side channel split in half with the lower portion disconnected at ~
434 $38.20 \text{ m}^3/\text{s}$. The side channel is shown from upstream (looking downstream, left image),
435 and close-up at the downstream disconnection (looking upstream, right image).

436 6. Discussion

437 Overall, areas identified as high stranding risk correspond to the same locations
438 where the most severe stranding events were observed in the study area. However,
439 exact fish counts were not taken and absence of stranding in other areas was not
440 explicitly documented. Thus, while these results provide encouraging qualitative
441 validation of the stranding risk analysis, future studies could more rigorously document
442 stranding occurrence (and absence) during downramping events to produce a

443 quantitative validation.

444 Habitat rehabilitation projects have modeled microhabitat (e.g., Koljonen et al.,
445 2013), scour potential (e.g., Elkins et al., 2007; Fischer et al., 2020) and bioenergetics
446 (Wheaton et al., 2018), but thus far not fish stranding risk. Unfortunately, creating
447 shallow landforms inevitably increases redd dewatering and fish stranding risks. If too
448 much of a regulated river's fish population is attracted to rehabilitated sites that are then
449 subjected to dewatering and stranding conditions at the wrong times, then the
450 population may decline, defeating project goals.

451 Project efforts may focus on discharges for targeted functionality, but ignore other
452 present flows impacting critical functions. This is especially of concern when river
453 rehabilitation projects and environmental flow regimes are designed independently by
454 different entities who are not collaborating. Parties designing projects need to be aware
455 of the entire flow regime, which is unlikely to change because of one rehabilitation
456 project yet could affect the success of that project.

457 6.1. Morphological impacts on stranding

458 Comparison of stranding risks across the three topographic conditions illustrates
459 how the Yuba Canyon Project and subsequent topographic changes affected stranding
460 risks. The most relevant topographic change was the creation of a series of side
461 channels running through the preexisting point bar. However, additional
462 morphodynamic changes occurred following completion of the project that increased
463 stranding risks. Because the flows modeled for this stranding risk analysis were not high
464 enough to initiate sediment transport (as indicated by model-derived Shields stresses,

465 direct observation, and past studies of augmented gravel migration in the reach (Brown
466 and Pasternack, 2014)), these changes are expected to have occurred on the falling
467 limb of much higher flows. Though morphodynamically relevant discharges were not
468 modeled for this study, comparison of stranding risks between fixed topographies still
469 illustrates the importance of morphodynamic processes altering stranding risks.

470 The lower side channel was originally designed to have a smoothly graded
471 connection to the mainstem at the downstream outlet, with a connection occurring from
472 the upstream end only at flood flows (i.e. $> 141.58 \text{ m}^3/\text{s}$). Thus, the lower side channel
473 was anticipated to gradually drain during flow reductions without the formation of
474 depressions which could potentially strand fish (Figure 6). Though the design
475 topography did not indicate stranding risk for the lower side channel, accumulation of
476 sediment near the downstream outlet following completion of the Yuba Canyon Project
477 formed a barrier between the side channel outlet and the river mainstem. Because this
478 side channel only had a single connection to the river mainstem, this resulted in
479 complete disconnection of the lower side channel at flows below $42.45 \text{ m}^3/\text{s}$. Flow from
480 the main channel is deflected by a vegetated gravel-cobble bar, creating a backflow
481 towards the side channel outlet (Figure 9). The rapid reduction in flow velocity
482 decreases sediment transport capacity, which may have led to the observed
483 accumulation of sediment at the outlet. The side channel's lack of an upstream
484 connection also prevents higher velocity flows from passing through which would
485 promote the sediment transport and scour necessary to keep the side channel open.
486 Flood pulses which allow overflow from upstream and induce scour play an important
487 role in maintaining side channels, and the lack of this scouring capacity can lead to the

488 formation of alluvial plugs (Constantine et al., 2010; Riquier et al., 2017). Once alluvial
489 plugs are established, side channels generally aggrade over time due to suspended
490 sediment deposition (Citterio and Piégay, 2009; Riquier et al., 2017). Furthermore, the
491 flow frequency in side channels has been found to be a strong predictor of side channel
492 sedimentation rates, with more rapid aggradation occurring in less frequently flowing
493 side channels (Citterio and Piégay, 2009; Riquier et al., 2017; van Denderen et al.,
494 2019b).

495 In contrast with the lower side channel, the upper side channel maintains both an
496 inlet and outlet connection at a discharge of 56.63 m³/s. Despite this fact, it was still
497 predicted to become disconnected by a flow reduction for both the design and post-
498 project topographies. This disconnection is due to its low gradient, leading to the
499 majority of the side channel having depths less than d_{min} before going dry. In this
500 situation, minute topographic variations cause the formation of pools that effectively trap
501 juvenile fish.

502 Due to the lack of fine sediments in the EDR, sedimentation dynamics in both side
503 channels are likely driven by bedload transport. For bedload-supplied side channels,
504 evidence suggests that aggradation could be mitigated by increasing the side channel's
505 width-to-depth ratio, as well as by shortening the length of the side channel relative to
506 the length of the main channel (van Denderen et al., 2019a).

507 Because both side channels were created on the inside of a meander bend, helical
508 flow may also be contributing to aggradation of the side channels. Helical flow caused
509 by river meandering creates a near-bed flow velocity component that is transverse to

510 the depth-averaged flow, leading to a disproportionate routing of sediment at
511 bifurcations. As a result, a greater proportion of sediment is routed towards the bifurcate
512 on the inside of a meander bend (Kleinhans et al., 2008; Hardy et al., 2011; van Dijk et
513 al., 2014). Because this effect is not resolved by the applied 2D hydrodynamic model,
514 the use of hydro-morphodynamic models and/or geomorphological considerations
515 would be necessary to determine the significance of this effect when designing side
516 channels.

517 Overall, this study illustrated that even if a side channel is designed to drain
518 positively, it may still pose significant stranding risks if it has low gradients or if alluvial
519 plugs form at inlets/outlets. Under a regulated flow regime, stranding risks in side
520 channels might be avoided by ensuring they remain inundated with active inlet and
521 outlet connections at minimum flows. Increased frequency of flow releases that
522 inundate the side channels could also help maintain active connections and prevent the
523 formation of alluvial plugs (Constantine et al., 2010, Riquier et al., 2017). However,
524 these very same measures would also likely diminish the habitat quality for rearing
525 juveniles, as they would be exposed to unsuitably high depths and velocities under such
526 conditions. To an extent, there may be a fundamental tradeoff between the amount of
527 quality rearing habitat and the presence of stranding risks for juvenile fish. The relative
528 impact of both factors should be considered as part of river rehabilitation project design,
529 as well as active management to effectively improve conditions for the target species.

530 6.2. Ramping rate effects on stranding risk

531 Ramping rates are not likely to be a dominant driver of juvenile Chinook salmon
532 stranding in the LYR. Because (i) the applied rate of change of discharge corresponds

533 to the highest levels experienced under current flow regulation practices, (ii) the flows
534 investigated are relatively low (where $\frac{\partial h}{\partial Q}$ is generally greatest), and (iii) the methods
535 used to estimate ramping rates do not consider wave attenuation, the estimated values
536 are expected to be upper bounds on the ramping rates experienced on the LZR. These
537 ramping rate estimates are much lower than those experienced in many hydropeaking
538 European rivers, staying near or below the target rates of <10-15 cm/hr suggested in
539 the literature for minimizing the effect of ramping rates on stranding risks (Halleraker et
540 al., 2003, 2007). Consequently, a focus on river topography, especially for recontouring
541 sites, is critical to managing stranding risk.

542 6.3. Other considerations

543 Typical water temperatures directly below Englebright Dam range between 7–13 °C,
544 coldest around February and warmest around July (RMT, 2010). Because spring-run
545 Chinook fry emergence begins in November, followed by fall-run Chinook salmon and
546 steelhead in the subsequent months, the coldest water temperatures experienced by
547 these juvenile salmonids typically occur during the same time period when fry are
548 smallest and most susceptible to stranding (Hunter, 1992). Additionally, ramping rate
549 has a greater impact on stranding under cold conditions (Bradford, 1997; Saltveit et al.,
550 2001; Halleraker et al., 2003). Consequently, the combination of relatively small
551 juveniles, cold temperatures (~6 °C), and moderate ramping rates (~10-15 cm/hr)
552 indicate that disconnecting habitat areas are expected to pose relatively greater
553 stranding risk during the winter in the EDR compared to those present during other
554 seasons or at locations further downstream. In contrast, ramping rates are not expected
555 to significantly impact stranding risks during the summer when waters are warmer and

556 juveniles are larger.

557 Regulated downramping on the LYR also typically occurs during the daytime, which
558 may elevate stranding risks for wild fish. However, hatchery fish could potentially strand
559 more in nighttime downramping scenarios (Saltveit et al., 2001). Because both wild and
560 hatchery fish are present on the LYR, the effect of time of day on stranding is uncertain.

561 7. Conclusions

562 More work is needed to further improve fish stranding prediction, but this study
563 showed promising results from applying a novel algorithm (available in well-documented
564 open-source software on GitHub) to a site known to have disconnections and fish
565 stranding. The algorithm successfully identified discharges at which different areas
566 become disconnected and confirmed the presence of high stranding risks in areas
567 where significant stranding was observed. The occurrence and severity of stranding
568 events were highly sensitive to topography and morphodynamic changes. In especially
569 active rivers, and particularly in artificially constructed features without any active self-
570 maintenance mechanisms, river morphology can change rapidly, in turn rapidly
571 changing stranding risks. Thus, as with most aspects of river science, the lack of
572 understanding of morphodynamic processes limits the applicability of these methods
573 presented to predict future conditions. Accurate characterization of stranding risks with
574 any method are inextricably dependent upon the availability and accuracy of
575 topographic data reflecting the present geomorphology. While the methodology
576 presented herein appears to be effective at delineating present stranding risks, it may
577 not capture the full extent of future stranding risks as morphodynamic changes alter a

578 design topography, as was the case for the lower side channel of the Yuba Canyon
579 Project. While the Yuba Canyon Project did create more spawning and rearing Chinook
580 salmon habitat, side channel disconnection also elevated stranding risks.

581 **Authorship contribution statement**

582 K.G. Larrieu: literature review, conceptualization, methodology, field work, software,
583 data analysis, original draft; G. B. Pasternack: conceptualization, 2D modeling and
584 ecohydraulics theory and practice, articulation about types of stranding, field work,
585 original draft editing, producing draft into journal manuscript, funding acquisition,
586 supervision, project administration.

587 **Declaration of Competing Interest**

588 The first author (Larrieu) declares that he has no known competing financial
589 interests or personal relationships that could have appeared to influence the work
590 reported in this paper. Larrieu was responsible for selecting model parameters, the
591 downramping flow regime, and conducting all data analysis with scientific
592 independence. The senior author (Pasternack) has had 17 years of science and
593 management involvement helping steward the lower Yuba River, possibly arising a
594 perception of conflict of interest, so disclosure is provided of activities relevant to this
595 section of the river. Pasternack was a UC Davis Principal Investigator on a Cooperative
596 Ecosystem Studies Unit collaboration with AFRP from 2003-2008 in which reports and
597 articles were written about the Englebright Dam reach (EDR). Pasternack was a paid
598 consultant for the multi-stakeholder Yuba Accord River Management Team to help
599 design and implement systemic ecohydraulic and geomorphic analysis of the LYR,

600 including EDR. Pasternack was a paid consultant for and later a UC Davis Principal
601 Investigator in a Cooperative Ecosystem Studies Unit collaboration with the US Army
602 Corps of Engineers to analyze gravel/cobble deficiency in the Englebright Dam Reach,
603 design a long-term gravel augmentation plan, and help implement the plan in its early
604 years. Pasternack was separately a paid consultant hired to undertake planning level
605 assessment of the number of spring-run Chinook salmon that could be supported by
606 river rehabilitation in the lower half of Englebright Dam Reach and in the Narrows
607 Reach. That consulting was funded by California Department of Water Resources and
608 Pacific Gas & Electric for their Habitat Expansion Agreement for Central Valley Spring
609 Run Chinook Salmon and California Central Valley Stealhead via subconsultancy
610 through ICF International, unrelated to and predating the AFRP project in this same
611 area. Pasternack was once again a UC Davis Principal Investigator on a Cooperative
612 Ecosystem Studies Unit collaboration with AFRP only during their early planning phase
613 for the Yuba Canyon Project, with the work limited to sharing public data with AFRP
614 consultants and having early planning discussions with AFRP consultants. Pasternack
615 had no involvement in the AFRP project thereafter (e.g., not in any AFRP pre-project
616 characterization, project design, or project implementation). Pasternack was a paid
617 consultant for Yuba Water Agency before and during this study to help apply scientific
618 research in Yuba River management broadly. YWA sought advice and analysis as to
619 the stranding events occurring at the Yuba Canyon project site. Consulting was done
620 independently of academic research following UC Davis policies and procedures.

621 **Supplementary materials**

622 Supplementary material associated with this article can be found on the journal's

623 website.

624 **Data Availability Statement**

625 The vast majority of the data used in this study is public domain data held by the
626 United States Fish and Wildlife Service Anadromous Fish Restoration Program. That
627 includes the original topography of the study site in 2017, the final project design
628 topography, and all SRH-2D model files for the AFRP project. We obtained these data
629 by sending an email request to the AFRP staff person assigned to the Yuba River,
630 which changes from time to time. The only data that we generated for this manuscript
631 was a new, post-project topographic map a year after construction (2019), which was
632 then put into the pre-existing SRH-2D models and run. These data are owned by the
633 project sponsor Yuba Water Agency, who determines availability. An email request for
634 that data may be submitted to Yuba Water Agency.

635 **Acknowledgments**

636 This work was funded by Yuba Water Agency (Marysville, California, USA; Awards
637 #201016094 and #19-000611). Authors made presentations to sponsor representatives
638 about research progress, but representatives did not direct or contribute to the new
639 methodology or model parameterization in this study. This project was also supported
640 by the USDA National Institute of Food and Agriculture, Hatch project number CA-D-
641 LAW-7034-H. We thank USFWS and its contractors for producing open, public datasets
642 and 2D models as well as sharing them for use in this project. We thank Duane Massa,
643 Loren Stearman, David Kowalik, and other staff from the Pacific States Marine Fisheries
644 Commission for assistance in field data collection. We thank Mark Grismer, Alexander

645 Forrest, Geoff Rabone, Paul Bratovich, Sebastian Schwindt, Morgan Neil, Dianne
646 Simodynes, Duane Massa, and Loren Stearman for discussions and/or manuscript draft
647 reviews.

648 **References**

- 649 Auer, S., Zeiringer, B., Führer, S., Tonolla, D., & Schmutz, S. (2017). Effects of river
650 bank heterogeneity and time of day on drift and stranding of juvenile European
651 grayling (*Thymallus thymallus* L.) caused by hydropeaking. *Science of the Total*
652 *Environment*, 575, 1515–1521. <https://doi.org/10.1016/j.scitotenv.2016.10.029>
- 653 Bauersfeld, K. (1978). Stranding of Juvenile Salmon by Flow Reductions at Mayfield
654 Dam on the Cowlitz River, 1976. Technical Report 36, Washington Department
655 of Fisheries.
- 656 Bell, M. C. (1991). *Fisheries Handbook of Engineering Requirements and Biological*
657 *Criteria* (3 ed.). Portland, Oregon. Retrieved from
658 [https://www.fs.fed.us/biology/nsaec/fishxing/fplibrary/Bell_1991_Fisheries_handb](https://www.fs.fed.us/biology/nsaec/fishxing/fplibrary/Bell_1991_Fisheries_handbook_of_engineering_requirements_and.pdf)
659 [ook_of_engineering_requirements_and.pdf](https://www.fs.fed.us/biology/nsaec/fishxing/fplibrary/Bell_1991_Fisheries_handbook_of_engineering_requirements_and.pdf)
- 660 Bradford, M. J. (1997). An experimental study of stranding of juvenile salmonids on
661 gravel bars and in sidechannels during rapid flow decreases. *Regulated Rivers:*
662 *Research and Management*, 13, 395-401. doi:10.1002/(SICI)1099-
663 1646(199709/10)13:5<395::AID-RRR464>3.0.CO;2-L
- 664 Brown, R. A., & Pasternack, G. B. (2009). Comparison of Methods for Analyzing
665 Salmon Habitat Rehabilitation Designs For Regulated Rivers. *River Research*
666 *and Applications*, 25, 745-772.
- 667 Brown, R. A., Pasternack, G. B. (2014). Hydrologic and topographic variability modulate
668 channel change in mountain rivers. *Journal of Hydrology*, 510, 551-564.
- 669 Brown, R. A., & Pasternack, G. B. (2019). How to build a digital river. *Earth-Science*

670 Reviews. doi:10.1016/j.earscirev.2019.04.028

671 Brown, R. A., Pasternack, G. B., & Lin, T. (2015). The topographic design of river
672 channels for form-process linkages for river restoration. *Environmental*
673 *Management*, 57(4), 929-942. doi:10.1007/s00267-015-0648-0

674 California Department of Fish and Wildlife. (2017). Standard Operating Procedure for
675 Critical Riffle Analysis for Fish Passage in California. Tech. rep., California
676 Department of Fish and Wildlife Instream Flow Program, Sacramento.

677 Chamberlain, W. H., & Wells, H. L. (1879). *History of Yuba County, California: With*
678 *Illustrations Descriptive of Its Scenery, Residences, Public Buildings, Fine Blocks*
679 *and Manufactories*. Thompson & West. Retrieved from
680 <https://books.google.com/books?id=i9MQnQEACAAJ>

681 Citterio, A., & Piégay, H. (2009). Overbank sedimentation rates in former channel lakes:
682 Characterization and control factors. *Sedimentology*, 56(2), 461-482.
683 doi:10.1111/j.1365-3091.2008.00979.x

684 Constantine, J. A., Dunne, T., Piégay, H., & Mathias Kondolf, G. (2010). Controls on the
685 alluviation of oxbow lakes by bed-material load along the Sacramento river,
686 California. *Sedimentology*, 57(2), 389-407. doi:10.1111/j.1365-
687 3091.2009.01084.x

688 Cushman, R. M. (1985). Review of ecological effects of rapidly varying flows
689 downstream from hydroelectric facilities. *North American Journal of Fisheries*
690 *Management*, 5(3A), 330-339.

691 Dijkstra, E. (1959). A note on two problems in connexion with graphs. *Numerische*
692 *Mathematik*, 1(1), 269–271.

693 Elkins, E. E., Pasternack, G. B., & Merz, J. E. (2007). The Use of Slope Creation for
694 Rehabilitating Incised, Regulated, Gravel-Bed Rivers. *Water Resources*
695 *Research*, 43: W05432. doi:10.1029/2006WR005159

- 696 Erwin, S. O., Jacobson, R. B., & Elliott, C. M. (2017). Quantifying habitat benefits of
697 channel reconfigurations on a highly regulated river system, Lower Missouri
698 River, USA. *Ecological Engineering*, 103(A), 59-75. doi:j.ecoleng.2017.03.004
- 699 Etherington, T. (2016). Least-Cost Modelling and Landscape Ecology: Concepts,
700 Applications, and Opportunities. *Curr Landscape Ecol Rep*, 1, 40-53.
701 doi:10.1007/s40823-016-0006-9
- 702 Evans, D. (2007). Effects of hypoxia on scope for activity and power capacity lake trout
703 (*Salvelinus namaycush*). *Canadian Journal of Fisheries and Aquatic Sciences*,
704 64, 345-361.
- 705 Federal Energy Regulatory Commission. (2019). Final Environmental Impact Statement
706 for Hydropower License, Yuba River Development Project: Project No. 2246-065
707 - California.
- 708 Fischer, J., Filip, G., Alford, L., Roseman, E., & Vaccaro, L. (2020). Supporting aquatic
709 habitat remediation in the Detroit River through numerical simulation.
710 *Geomorphology*, 353, 107001.
- 711 Flodmark, L. E., Urke, H. A., Halleraker, J. H., Arnekleiv, J. V., Vøllestad, L. A., & Poléo,
712 A. B. (2002). Cortisol and glucose responses in juvenile brown trout subjected to
713 a fluctuating flow regime in an artificial stream. *Journal of Fish Biology*, 60(1),
714 238-248. doi:10.1006/jfbi.2001.1845
- 715 Halleraker, J. H., Saltveit, S. J., Harby, A., Arnekleiv, J. V., Fjeldstad, H. P., & Kohler, B.
716 (2003). Factors influencing stranding of wild juvenile brown trout (*Salmo trutta*)
717 during rapid and frequent flow decreases in an artificial stream. *River Research*
718 *and Applications*, 19, 589-603. doi:10.1002/rra.752
- 719 Halleraker, J. H., Sundt, H., Alfredsen, K. T., & Dangelmaier, G. (2007). Application of
720 Multiscale Environmental Flow Methodologies As Tools for Optimized
721 Management of a Norwegian Regulated National Salmon Watercourse. *River*
722 *Research and Applications*, 23, 493-510. doi:10.1002/rra.1000

- 723 Hardy, R. J., Lane, S. N., & Yu, D. (2011). Flow structures at an idealized bifurcation: A
724 numerical experiment. *Earth Surface Processes and Landforms*, 36(15), 2083-
725 2096. doi:10.1002/esp.2235
- 726 Harrison, L. R., Bray, E., Overstreet, B., Legleiter, C. J., Brown, R. A., Merz, J. E.,
727 Bond, R. M., Nicol, C. L., & Dunne, T. (2019). Physical controls on salmon redd
728 site selection in restored reaches of a regulated, gravel-bed river. *Water*
729 *Resources Research*, 55(11), 8942-8966.
- 730 Hauer, C., Unfer, G., Holzapfel, P., Haimann, M., & Habersack, H. (2014). Impact of
731 channel bar form and grain size variability on estimated stranding risk of juvenile
732 brown trout during hydropeaking. *Earth Surface Processes and Landforms*, 39,
733 1622-1641. doi:10.1002/esp.3552
- 734 Hunter, M. A. (1992). Hydropower flow fluctuations and salmonids: A review of the
735 biological effects, mechanical causes, and options for mitigation. Technical
736 Report No. 119, Department of Fisheries, State of Washington.
- 737 Irvine, R. L., Thorley, J. L., Westcott, R., Schmidt, D., & Derosa, D. (2014). Why Do Fish
738 Strand? An Analysis of Ten Years of Flow Reduction Monitoring Data From the
739 Columbia and Kootenay Rivers, Canada. *River Research and Applications*, 31,
740 1242-1250. doi:10.1002/rra
- 741 Juárez, A., Adeva-Bustos, A., Alfredsen, K., & Dønnum, B. O. (2019). Performance of a
742 two-dimensional hydraulic model for the evaluation of stranding areas and
743 characterization of rapid fluctuations in hydropeaking rivers. *Water (Switzerland)*,
744 11. doi:10.3390/w11020201
- 745 Katopodis, C., & Gervais, R. (2016). Fish swimming performance database and
746 analyses. DFO Can. Sci. Advis. Sec. Res. Doc. 2016/002.
- 747 Kauffman, J., Beschta, R., Otting, N., & Lytjen, D. (1997). An ecological perspective of
748 riparian and stream restoration in the western United States. *Fisheries*, 22(5), 12-
749 24.

- 750 Kleinhans, M. G., Jagers, H. R., Mosselman, E., & Sloff, C. J. (2008). Bifurcation
751 dynamics and avulsion duration in meandering rivers by one-dimensional and
752 three-dimensional models. *Water Resources Research*, 44(8): W08454.
753 doi:10.1029/2007WR005912
- 754 Koljonen, S., Huusko, A., Mäki-Petäys, A., Louhi, P., & Muotka, T. (2013). Assessing
755 habitat suitability for juvenile Atlantic salmon in relation to in-stream restoration
756 and discharge variability. *Restoration ecology*, 21(3), 344-352.
- 757 Lai, Y. G. (2008). SRH-2D version 2: Theory and User Manual. US Dept. of the Interior,
758 Bureau of Reclamation, Technical Service Center, Denver, Co.
- 759 Larrieu, K. G., Pasternack, G. B., & Schwindt, S. (2020). Automated analysis of lateral
760 river connectivity and fish stranding risks—Part 1: Review, theory and algorithm.
761 *Ecohydrology*, 14(2), e226. doi: 10.1002/eco.2268
- 762 McElroy, B., DeLonay, A., & Jacobson, R. (2012). Optimum swimming pathways of fish
763 spawning migrations in rivers. *Ecology*, 93, 29-34. doi:10.1890/11-1082.1
- 764 Meybeck, M. (2003). Global analysis of river systems: From Earth system controls to
765 Anthropocene syndromes. *Philosophical Transactions of the Royal Society B:
766 Biological Sciences*, 358, 1935-1955. doi:10.1098/rstb.2003.1379
- 767 Moniz, P. J., Pasternack G, B., Massa D, A., Stearman L, W., & Bratovich P, M. (2019).
768 Do rearing salmonids predictably occupy physical microhabitat? *Journal of
769 Ecohydraulics*, 1-19. doi:10.1080/24705357.2019.1696717
- 770 Morandi, B., Piégay, H., Lamouroux, N., & Vaudor, L. (2014). How is success or failure
771 in river restoration projects evaluated? Feedback from French restoration
772 projects. *Journal of Environmental Management*, 137, 178-188.
- 773 Moyle, P. B., Katz, J. V., & Quiñones, R. M. (2011). Rapid decline of California's native
774 inland fishes: A status assessment. *Biological Conservation*, 144, 2414-2423.
775 doi:10.1016/j.biocon.2011.06.002

- 776 Noack, M., & Schneider, M. (2009). Impacts of Hydropeaking on Juvenile Fish Habitats:
777 a Qualitative and Quantitative Evaluation Using the Habitat Model CASiMiR. 7th
778 International Symposium on Ecohydraulics.
- 779 Noack, M., Schneider, M., & Wieprecht, S. (2013). The habitat modelling system
780 CASiMiR: A multivariate fuzzy approach and its applications. In *Ecohydraulics:
781 An integrated approach*, John Wiley & Sons, Ltd. Chichester, UK (pp. 75-92).
782 doi:10.1002/9781118526576.ch4
- 783 Pacific States Marine Fisheries Commission. (2019). Yuba River Accord M&E Field
784 Update, January 8, 2019, Additional Submittal.
- 785 Paillex, A., Dolédec, S., Castella, E., & Mérioux, S. (2009). Large river floodplain
786 restoration: predicting species richness and trait responses to the restoration of
787 hydrological connectivity. *Journal of Applied Ecology*, 46, 250-258.
788 doi:10.1111/j.1365-2664.2008.01593.x
- 789 Palmer, M., Menninger, H., & Bernhardt, E. (2010). River restoration, habitat
790 heterogeneity and biodiversity: a failure of theory or practice? *Freshwater
791 Biology*, 55, 205-222.
- 792 Pasternack, G. B. (2019). *Applied Fluvial Ecohydraulics*. Oxford Bibliographies in
793 Environmental Science. (E. Wohl, Ed.) New York: Oxford University Press.
794 doi:10.1093/OBO/9780199363445-0124
- 795 Pasternack, G. B. (2020). River Restoration: Disappointing, Nascent, Yet Desperately
796 Needed. Reference Module in Earth Systems and Environmental Sciences,
797 Elsevier, doi: 10.1016/B978-0-12-409548-9.12449-2
- 798 Pasternack, G. B., & Brown, R. (2013). Ecohydraulic design of riffle-pool relief and
799 morphological-unit geometry in support of regulated gravel-bed river
800 rehabilitation. In I. Maddock, A. Harby, P. Kemp, & P. Wood (Eds.),
801 *Ecohydraulics: an integrated approach* (pp. 337-355). Chichester, UK: John
802 Wiley & Sons, Ltd.

803 Pasternack, G. B., Fulton, A. A., & Morford, S. L. (2010). Yuba river analysis aims to aid
804 spring-run chinook salmon habitat rehabilitation. *California Agriculture*, 64, 69-77.
805 doi:10.3733/ca.v064n02p69

806 Person, E. (2013). *Impact of Hydropeaking on Fish and their Habitat* (Doctoral Thesis).
807 École Polytechnique Fédérale de Lausanne, Lausanne.
808 <https://doi.org/10.5075/epfl-thesis-5812>

809 Quinn, T. P., & Buck, G. B. (2001). Size- and Sex-Selective Mortality of Adult Sockeye
810 Salmon: Bears, Gulls, and Fish Out of Water. *Transactions of the American*
811 *Fisheries Society*, 130, 995-1005. doi:10.1577/1548-
812 8659(2001)130<0995:sassmo>2.0.co;2

813 Richmond, M. C., & Perkins, W. A. (2009). Efficient calculation of dewatered and
814 entrapped areas using hydrodynamic modeling and GIS. *Environmental*
815 *Modelling and Software*, 24, 1447-1456. doi:10.1016/j.envsoft.2009.06.001

816 Riquier, J., Piégay, H., Lamouroux, N., & Vaudor, L. (2017). Are restored side channels
817 sustainable aquatic habitat features? Predicting the potential persistence of side
818 channels as aquatic habitats based on their fine sedimentation dynamics.
819 *Geomorphology*, 295, 507-528. doi:10.1016/j.geomorph.2017.08.001

820 RMT. (2010). *LYR Water Temperature Objectives*. Tech. rep., LYR Accord River
821 Management Team Planning Group. Retrieved from
822 [http://www.yubaaccordrmt.com/Studies Reports/LYR Water Temp Objectives](http://www.yubaaccordrmt.com/Studies Reports/LYR Water Temp Objectives Tech Memo.pdf)
823 [Tech Memo.pdf](http://www.yubaaccordrmt.com/Studies Reports/LYR Water Temp Objectives Tech Memo.pdf)

824 Rosenfeld, J. S., Raeburn, E., Carrier, P. C., & Johnson, R. (2008). Effects of Side
825 Channel Structure on Productivity of Floodplain Habitats for Juvenile Coho
826 Salmon. *North American Journal of Fisheries Management*, 28(4), 1108-1119.
827 doi:10.1577/M07-027.1

828

829 Sabo, M., Bryan, C., Kelso, W., & Rutherford, D. (1999). Hydrology and aquatic habitat

830 characteristics of a riverine swamp: II hydrology and the occurrence of chronic
831 hypoxia. *Regulated Rivers: Research & Management*, 15, 525-542.

832 Saltveit, S. J., Halleraker, J. H., Arnekleiv, J. V., & Harby, A. (2001). Field experiments
833 on stranding in juvenile atlantic salmon (*Salmo salar*) and brown trout (*Salmo*
834 *trutta*) during rapid flow decreases caused by hydropeaking. *Regulated Rivers:*
835 *Research & Management*, 17, 609-622. doi:10.1002/rrr.652.abs

836 Schwindt, S., Larrieu, K. G., Pasternack, G., & Rabone, G. (2020). *River Architect.*
837 *SoftwareX*. doi:10.1016/j.softx.2020.100438

838 Silva, P., & Pasternack, G. (2018). 2017 LYR Topographic Mapping Report. Prepared
839 for the Yuba Water Agency. University of California, Davis.

840 Snyder, N. P., Rubin, D. M., Alpers, C. N., Childs, J. R., Curtis, J. A., Flint, L. E., &
841 Wright, S. A. (2004). Estimating accumulation rates and physical properties of
842 sediment behind a dam: Englebright Lake, Yuba River, northern California.
843 *Water Resour. Res.*, 40, W11301. doi:10.1029/2004WR003279

844 Sommer, T. R., Harrell, W. C., & Nobriga, M. L. (2005). Habitat Use and Stranding Risk
845 of Juvenile Chinook Salmon on a Seasonal Floodplain. *North American Journal*
846 *of Fisheries Management*, 25, 1493-1504. doi:10.1577/m04-208.1

847 Tuhtan, J. A., Noack, M., & Wieprecht, S. (2012). Estimating Stranding Risk due to
848 Hydropeaking for Juvenile European Grayling Considering River Morphology.
849 *KSCE Journal of Civil Engineering*, 16(2), 197-206. doi:10.1007/s12205-012-
850 0002-5

851 van Denderen, R. P., Schielen, R. M., Straatsma, M. W., Kleinhans, M. G., & Hulscher,
852 S. J. (2019a). A characterization of side channel development. *River Research*
853 *and Applications*, 35(9), 1597-1603. doi:10.1002/rra.3462

854 van Denderen, R. P., Schielen, R. M., Westerhof, S. G., Quartel, S., & Hulscher, S. J.
855 (2019b). Explaining artificial side channel dynamics using data analysis and
856 model calculations. *Geomorphology*, 327, 93-110.

857 doi:10.1016/j.geomorph.2018.10.016

858 van Dijk, W. M., Schuurman, F., Van de Lageweg, W. I., & Kleinhans, M. G. (2014).
859 Bifurcation instability and chute cutoff development in meandering gravel-bed
860 rivers. *Geomorphology*, 213, 277-291. doi:10.1016/j.geomorph.2014.01.018

861 Vanzo, D., Tancon, M., Zolezzi, G., Alfredsen, K., & Siviglia, A. (2016). Modeling
862 Approach for the Quantification of Fish Stranding Risk: the Case of Lundesokna
863 River (Norway). 11th International Symposium on Ecohydraulics, 1-9.

864 Wheaton, J. M., Pasternack, G. B., and Merz, J. E. 2004. Spawning Habitat
865 Rehabilitation - 1. Conceptual Approach & Methods. *International Journal of*
866 *River Basin Management* 2:1:3-20.

867 Wheaton, J., Bouwes, N., Mchugh, P., Saunders, C., Bangen, S., Bailey, P., . . . Jordan,
868 C. (2018). Upscaling site-scale ecohydraulic models to inform salmonid
869 population-level life cycle modeling and restoration actions—Lessons from the
870 Columbia River Basin. *Earth Surface Processes and Landforms*, 43(1), 21-44.

871 Yoshiyama, R. M., Fisher, F. W., & Moyle, P. B. (1998). Historical Abundance and
872 Decline of Chinook Salmon in the Central Valley Region of California. *North*
873 *American Journal of Fisheries Management*, 18, 487-521. doi:10.1577/1548-
874 8675(1998)018<0487:haadoc>2.0.co;2

1 **Automated analysis of river habitat connectivity and fish stranding risks. Part 2:**
2 **juvenile Chinook salmon stranding at river rehabilitation site**

3

4

Supplementary Materials

5

6 **1 Floodplain interpolation accuracy**

7 Extrapolation accuracy was tested on 2D model WSE results for the lower Yuba
8 River (Hopkins and Pasternack, 2017). WSE values in the main channel were used as
9 training data, while side channels, backwaters, and other ponded areas were used for
10 testing. The choice of training and testing data was made to be more representative of
11 typical WSE extrapolation than randomized cross-validation. A randomized cross-
12 validation was also performed, which yielded lower errors than those presented herein
13 due to generally greater geographic proximity of training and testing points. Overall, the
14 extrapolated wetted areas exhibited a qualitatively good match to the original data
15 (**Table 1**), considering that the median error is comparable to uncertainty in WSE
16 prediction from 2D modeling of the 37-km lower Yuba River segment as a whole.
17 Specifically, in comparing 2.1 million airborne LiDAR observed vs 2D model predicted
18 WSEs at a summer baseflow, 69% were within ± 6.1 cm, which is very good
19 performance for meter-resolution modeling of such a long domain.

20

21 **Table 1:** Median signed and unsigned errors for each interpolation method tested.

Method	Median signed error (cm)	Median unsigned error (cm)
Nearest Neighbor	-5.89	9.41
Inverse Distance Weighted	-3.74	7.68
Ordinary Kriging	-5.23	8.35
Empirical Bayesian Kriging	-2.67	8.16

22

23 **2 Yuba Canyon model details**

24 *2.1 Model boundary conditions*

25 The Yuba Canyon Project's stage-discharge rating curve was developed using WSE
26 values collected from a pressure transducer and discharge values taken as a time-
27 lagged sum of YRS and DCS gage readings. WSE was then fitted as a function of
28 discharge for flows up to 226.40 m³/s (8,000 cfs) using a fourth order polynomial. This
29 function was adapted to set boundary conditions for all model simulations. A constant
30 inflow of 1.22 m³/s (43 cfs) was included at the Deer Creek tributary. This value was
31 chosen as the median recorded flow at the DCS gage since the beginning of Deer
32 Creek regulation and during the season of interest for juvenile Chinook salmon rearing
33 (Feb 1 - June 15).

34

35

36

37

38 **Table 2:** Inlet discharges and outlet water surface elevations used to set boundary
39 conditions for the SRH-2D models.

Yuba River Inflow (cfs)	Deer Creek Inflow (cfs)	Outlet WSE (ft)
500	43	270.167
600	43	270.354
700	43	270.534
800	43	270.708
900	43	270.876
1000	43	271.038
1100	43	271.194
1200	43	271.345
1300	43	271.491
1400	43	271.632
1500	43	271.768
1600	43	271.899
1800	43	272.149
2000	43	272.383

40

41 2.2 2D model validation

42 Extensive SRH-2D hydraulic validation has been done in EDR (Brown and
43 Pasternack, 2012, 2013) to evaluate mass conservation, WSE (15,135 observations),
44 velocity magnitude (2,141 observations), and velocity direction (1,743 observations).
45 For example, the coefficient of variation between predicted and observed velocity
46 magnitudes was 0.76 and 0.85 for the 2012 and 2013 studies, respectively. A thorough
47 analysis of recirculating eddy prediction was also reported. All validation results were at
48 or above peer-reviewed journal article standards for 2D modeling. Furthermore, model
49 accuracy was vetted through bioverification of Chinook salmon spawning habitat
50 predictions against observed spawning locations with an excellent outcome.

51 Because this study used the same model in the same resolution for similar flows as
52 previous validation was done, extensive validation work was not necessary.
53 Nevertheless, WSE was particularly important because it controls disconnection. Post-
54 project WSE measurements taken near the water's edge at the Yuba Canyon site
55 showed a small mean absolute error of 3.1 cm (0.1 ft).

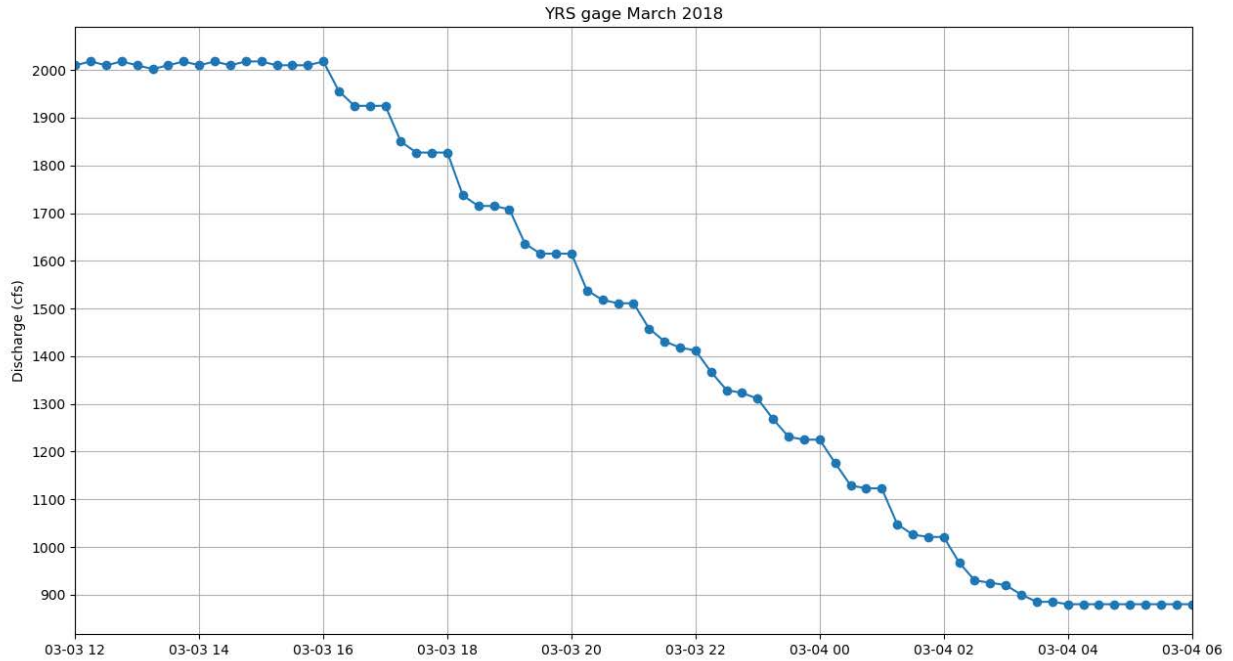
56 Survey points were also taken with a Trimble R8 real-time kinematic global
57 positioning system unit at the water's edge when side channels were disconnected.
58 This data was compared with corresponding interpolated depth rasters. Wetted areas
59 delineated by the IDW interpolation showed agreement within one pixel for nearly all
60 such points collected.

61

62 **3 Flow downramping**

63 Fifteen-minute resolution Yuba-Smartsville (YRS) gage readings were analyzed in
64 order to characterize relevant downramping scenarios during juvenile spring-run
65 Chinook salmon rearing on the lower Yuba River. Figures 1 and 2 illustrate
66 characteristic flow reductions used to determine a characteristic downramping rate of
67 7.07 cms/hr (250 cfs/hr).

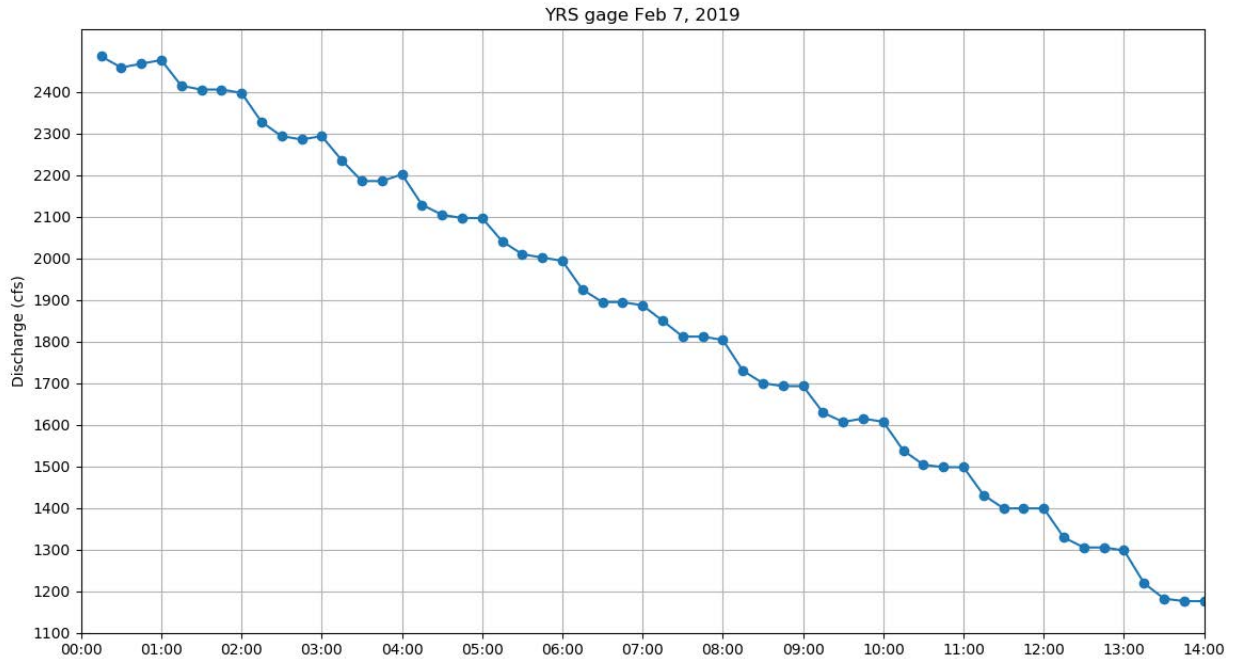
68



69

70 **Figure 1:** A flow reduction during March 2018. All points correspond to measurements
 71 recorded 15 minutes apart. Note that each hour consists of a ~100 cfs flow reduction
 72 over 30 minutes, followed by 30 minutes of constant flows.

73



74

75 **Figure 2:** Another flow reduction during February 2019. Again, note that each hour
 76 consists of a 100 cfs flow reduction within 30 minutes, followed by 30 minutes of
 77 constant flows.

78

79 **4 References**

80 Brown, R. A., & Pasternack, G. B. (2012). Monitoring and assessment of the 2010-2011
 81 gravel/cobble augmentation in the Eglebright Dam Reach of the LYR. University
 82 of California, Davis. Prepared for US Army Corps of Engineers, Sacramento
 83 District.

84 Brown, R. A., & Pasternack, G. B. (2013). Monitoring and assessment of gravel/cobble
 85 augmentation in the Eglebright dam reach of the lower Yuba River, CA:
 86 11/01/2011 to 12/1/2012. Prepared for the U. S. Army Corps of Engineers,

87 Sacramento District.

88 Hopkins, C. E., & Pasternack, G. B. (2017). *Autumn 2014 LYR TUFLOW GPU 2D*

89 *Model Description and Validation*. Prepared for Yuba County Water Agency.

90 University of California, Davis, CA.

91

92

93